Atmospheric
Chemistry
and Physics

Open Access

Discussions

WAIS Divide ice core suggests sustained changes in the atmospheric formation pathways of sulfate and nitrate since the 19th century in the extratropical Southern Hemisphere

E. D. Sofen[1], B. Alexander[1], E. J. Steig[2], M. H. Thiemens[3], S. A. Kunasek[2], H. M. Amos[1,*], A. J. Schauer[2], M. G. Hastings[1,**], J. Bautista[2], T. L. Jackson[3], L. E. Vogel[4], J. R. McConnell[5], D. R. Pasteris[5], and E. S. Saltzman[6]

[1]Department of Atmospheric Sciences, University of Washington, Seattle, WA 98195, USA
[2]Department of Earth and Space Sciences, University of Washington, Seattle, WA 98195, USA
[3]University of California at San Diego, La Jolla, CA 92093, USA
[4]Joint Institute for the Study of the Atmosphere and the Ocean, University of Washington, Seattle, WA 98195, USA
[5]Division of Hydrologic Sciences, Desert Research Institute, Reno, NV 89512, USA

ACPD

13, 23089–23138, 2013

WAIS Divide sulfate and nitrate isotopes

E. D. Sofen et al.

Title Page	
Abstract	Introduction
Conclusions	References
Tables	Figures
◄◄	►►
◄	►
Back	Close
Full Screen / Esc	
Printer-friendly Version	
Interactive Discussion	

[6]Department of Earth System Science, University of California at Irvine, Irvine, CA 92697, USA

[*]now at: Department of Earth and Planetary Sciences, Harvard University, Cambridge, MA 02138, USA

[**]now at: Department of Geological Sciences, Brown University, Providence, RI 02912, USA

Correspondence to: E. D. Sofen (esofen@atmos.uw.edu)

E. D. Sofen et al.

Title Page

Abstract | Introduction

Conclusions | References

Tables | Figures

|◄ | ►|

◄ | ►

Back | Close

Full Screen / Esc

Printer-friendly Version

Interactive Discussion

Abstract

The triple-oxygen isotopic composition ($\Delta^{17}O = \delta^{17}O - 0.52 \times \delta^{18}O$) of sulfate and nitrate reflects the relative importance of their different production pathways in the atmosphere. A new record of sulfate and nitrate $\Delta^{17}O$ spanning the last 2400 yr from the West Antarctic Ice Sheet Divide ice core project shows significant changes in both sulfate and nitrate $\Delta^{17}O$ in the most recent 200 yr, indicating changes in their formation pathways. The sulfate $\Delta^{17}O$ record suggests that an additional 12–18 % of sulfate formation occurs via aqueous-phase production by O_3, relative to that in the gas-phase in the present-day compared to the early 19th century. Nitrate $\Delta^{17}O$ indicates a increasing importance of RO_2 in NO_x-cycling between the mid-19th century and present-day in the mid-to-high latitude Southern Hemisphere. The former has implications for the climate impacts of sulfate aerosol, while the latter has implications for the tropospheric O_3 production rate in remote low-NO_x environments. Using other ice core observations, we rule out drivers for these changes other than variability in extratropical oxidant (OH, O_3, RO_2, H_2O_2, and reactive halogens) concentrations. However, assuming OH, H_2O_2, and O_3 are the main oxidants contributing to sulfate formation, Monte Carlo box model simulations require a large (≥ 210 %) increase in the $[O_3]/[OH]$ ratio over the Southern Ocean in the early 19th century to match the sulfate $\Delta^{17}O$ record. This unlikely scenario points to a deficiency in our understanding of sulfur chemistry and suggests other oxidants may play an important role in sulfate formation in the mid-to-high latitude marine boundary layer. The observed decrease in nitrate $\Delta^{17}O$ since $\sim$ 1860 CE is most likely due to an increased importance of RO_2 over O_3 in NO_x-cycling and can be explained by a 48–84 % decrease in the $[O_3]/[RO_2]$ ratio in the extratropical Southern Hemisphere NO_x-source regions.

1   Introduction

The formation pathways of tropospheric sulfate (SO_4^{2-}) and nitrate (NO_3^-) impact atmospheric chemistry and climate in a number of ways. The importance of gas-phase vs. aqueous-phase sulfate formation will impact the contribution of sulfate aerosols to direct scattering of solar radiation and indirect radiative effects via changes in cloud microphysics. Gas-phase SO_4^{2-} production has the potential to increase sulfate aerosol and CCN concentrations (Langner et al., 1992), while aqueous-phase production in existing droplets can enhance the ability of those particles to act as CCN at lower supersaturations (Kaufman and Tanre, 1994). Changes in nitrogen oxides ($NO_x = NO + NO_2$) cycling and nitrate aerosol formation impact O_3 production rates and the lifetime of NO_x, with implications for the oxidizing capacity of the atmosphere. Oxygen isotope measurements from ice cores can provide insight into the formation pathways of sulfate and nitrate aerosol and how they change over time. Quantitatively connecting changes in the oxygen isotopes of sulfate and nitrate to changes in atmospheric conditions remains a key challenge in the application of these measurements to paleo-chemistry.

A key control on the formation pathways of sulfate and nitrate is the abundance of oxidants involved in their formation. Atmospheric oxidants such as ozone (O_3) and the hydroxyl radical (OH) play a central role in determining the chemical makeup of the troposphere, as their concentrations determine the lifetime and fate of reduced trace gases and the formation of aerosols including sulfate and nitrate, with implications for climate and air pollution. Atmospheric oxidant concentrations are strongly influenced by emissions of O_3 precursors such as carbon monoxide (CO), methane (CH_4), volatile organic carbon (VOC) species, and nitrogen oxides, and are fundamentally coupled to each other via oxidant cycling. Reactive halogens (e.g. BrO) also impact the chemistry of oxidants, sulfate, and nitrate in a number of ways (von Glasow et al., 2004; Morin et al., 2007; Saiz-Lopez and von Glasow, 2012).

Our knowledge of past variability in the abundance of atmospheric oxidants is very limited. Global chemical transport models (CTM) have been used to investigate oxidant

changes based on emissions changes between the preindustrial (prior to 1750, 1800, or 1850 CE) and the present-day (between 1990 and 2010 CE). Most models suggest an increase in global tropospheric O_3 (+25 % to +63 %), an even larger increase in H_2O_2 (+44 % to +130 %), and no consistent agreement in the sign or magnitude of the change in OH (−33 % to +14 %), although most suggest OH has decreased slightly (Sofen et al., 2011; John et al., 2012, and references therein). These global averages largely reflect changes in the tropics and Northern midlatitudes where oxidant concentrations are highest. The lifetime of CH_4, which is controlled by OH, is also largely determined in the tropics (Holmes et al., 2013). However, the abundance and isotopic composition of shorter-lived species such as sulfate and nitrate preserved in Antarctic ice cores is determined by processes in mid-to-high southern latitudes. Ice core measurements of hydrogen peroxide (H_2O_2) indicate a ∼ 50 % increase in its Antarctic boundary layer concentration during the 20th c. due to a combination of the large-scale influence of increases in CO and CH_4 emissions and the local increase in tropospheric O_3 photolysis (producing HO_2, a precursor of H_2O_2) over Antarctica due to the stratospheric ozone hole since the 1970s (Lamarque et al., 2011). Late 19th c. measurements of surface O_3 using the Schönbein method suggest very low preindustrial surface [O_3] around $10\,nmol\,mol^{-1}$ (Sandroni et al., 1992; Pavelin et al., 1999) at a number of sites in both hemispheres, implying that human activity in the 20th c. has increased surface [O_3] by ∼ 100 % in remote regions, although there is considerable uncertainty surrounding the reconstruction of these historic measurements. Because oxidants are generally not well-preserved in any paleo-archive, there is no other direct evidence of the magnitude of past oxidant changes. The triple oxygen isotopes of sulfate and nitrate from ice cores have been suggested as a potential constraint on local to regional paleo-oxidant changes because the sulfate and nitrate preserve the isotopic composition of the oxidants involved in their formation. However, their interpretation is complicated by other factors influencing sulfate and nitrate chemistry and uncertainty in the spatial scale reflected by measurements at a single location.

The first measurements of the triple-oxygen isotopes of sulfate from the West Antarctic Ice Sheet (WAIS) Divide ice coring project (http://www.waisdivide.unh.edu/) spanning 1774–2005 CE show an increase in the early 19th c., with stable values from the mid-19th c. to present (Kunasek et al., 2010). The lack of change since the mid-1800s is consistent with increases in both O_3 and H_2O_2, because they have offsetting effects on the sulfate isotopes (Kunasek et al., 2010; Sofen et al., 2011). The present work extends this record back another 2000 yr and includes the complementary measurement of nitrate isotopes. We compare these isotope records to other ice core chemical records and consider possible explanations for the observed variability in the $\Delta^{17}O$ record.

2 Background

The ^{17}O-excess ($\Delta^{17}O = \delta^{17}O - 0.52 \times \delta^{18}O$) is a measure of the deviation from mass-dependent fractionation of $\delta^{17}O$ and $\delta^{18}O$. The formation of ozone produces a large positive $\Delta^{17}O$ (Thiemens and Heidenreich, 1983) that is then passed to other atmospheric species through oxidation reactions (Thiemens, 2006).

The mean observed $\Delta^{17}O(O_3)$ = 25 ‰ (Krankowsky et al., 1995; Johnston and Thiemens, 1997), but measurements using cryogenic trapping of O_3 are complicated by low O_3 abundances and potential for contamination by atmospheric O_2 which can bias $\Delta^{17}O(O_3)$ low (Brenninkmeijer et al., 2003). However, recent measurements at one location using a different method find $\Delta^{17}O(O_3)$ = 22.9 ± 1.9 ‰, consistent with previous observations (Vicars et al., 2012). Model calculations (Lyons, 2001) based on laboratory-measured rate constants indicate $\Delta^{17}O(O_3)$ = 35 ‰, which is within the range of observations (Krankowsky et al., 1995; Johnston and Thiemens, 1997). Because of the possible low bias in the observations, studies of sulfate or nitrate $\Delta^{17}O$ have assumed $\Delta^{17}O(O_3)$ of 25 ‰ to 35 ‰ (Michalski et al., 2003; Morin et al., 2007; Kunasek et al., 2010; Morin et al., 2011; Sofen et al., 2011; Alexander et al., 2012). A global modeling study suggests that $\Delta^{17}O(O_3)$ = 35 ‰ agrees best with observations

E. D. Sofen et al.

Title Page

Abstract	Introduction
Conclusions	References
Tables	Figures

|◀ | ▶|

◀ | ▶

Back | Close

Full Screen / Esc

Printer-friendly Version

Interactive Discussion

of $\Delta^{17}O(NO_3^-)$ globally (Alexander et al., 2009). Observations show $\Delta^{17}O(H_2O_2) =$ 1.3 ± 0.3 ‰ (Savarino and Thiemens, 1999). Generally, $\Delta^{17}O(OH) = 0$ ‰ due to rapid isotopic exchange with water vapor (Dubey et al., 1997; Lyons, 2001), but in polar regions where water vapor concentrations are low, OH may retain a small fraction of the positive $\Delta^{17}O$ acquired from O_3 (Morin et al., 2007). Observations show $\Delta^{17}O(O_2) = -0.34$ ‰ (Barkan and Luz, 2005).

Sulfate and nitrate both acquire a mass-independent (non-zero $\Delta^{17}O$) oxygen isotopic composition from the oxidants involved in their formation. The main oxidants relevant to nitrate formation are O_3, RO_2 (R = H atom or organic group), OH, and BrO, while sulfate formation involves primarily O_3, H_2O_2, and OH. Hypohalous acids (HOCl and HOBr) may also be important oxidants for sulfate formation in the marine boundary layer (Vogt et al., 1996; von Glasow et al., 2002), but the rate constant for the reactions $HOBr/HOCl + HSO_3^-$ are unknown (Liu, 2002). Sulfate and nitrate $\Delta^{17}O$ is influenced solely by the relative importance of their formation pathways (Savarino et al., 2000; Michalski et al., 2003), which depends upon the relative abundance of the different oxidants, the isotopic composition of each oxidant, and the number of oxygen atoms transferred during oxidation.

2.1 Sulfate chemistry and $\Delta^{17}O$

While anthropogenic emissions dominate the present-day Northern Hemisphere sulfur budget, marine biogenic emissions of dimethyl sulfide (DMS) and sea salt sulfate represent the majority of Southern Hemisphere sulfur emissions (Bates et al., 1992; Seinfeld and Pandis, 2006). Poleward of $\sim 35°$ S, > 75 % of sulfur emissions are from marine sources (Spiro et al., 1992). Most DMS is oxidized by OH, NO_3, and BrO to SO_2 and then to SO_4^{2-}, and most of the remainder forms methanesulfonic acid (MSA). The yield of MSA relative to SO_2 from DMS oxidation is enhanced at lower temperatures (Arsene et al., 1999) or when the oxidant is BrO rather than OH (Read et al., 2008).

WAIS Divide sulfate and nitrate isotopes

E. D. Sofen et al.

Title Page

Abstract | Introduction

Conclusions | References

Tables | Figures

|◄ | ►|

◄ | ►

Back | Close

Full Screen / Esc

Printer-friendly Version

Interactive Discussion

The main tropospheric sulfate formation pathways are summarized in Fig. 1a. The rate of sulfate production by each oxidation pathway is determined by oxidant concentrations and several other factors. SO_2 is oxidized by OH in the gas phase, forming sulfuric acid (H_2SO_4). SO_2 may also dissolve into cloud droplets, speciating into S(IV)

(= $SO_2 \cdot H_2O + HSO_3^- + SO_3^{2-}$), where it may react with H_2O_2, O_3, hypohalous acids (HOCl or HOBr) or O_2 (catalyzed my transition metals Fe(III) and Mn(II)) to form sulfate. Cloud cover and liquid water content impacts the relative importance of gas vs. aqueous-phase sulfate production. Cloud water pH influences S(IV) speciation and therefore the sulfate production rate by O_3. Finally, heterogeneous sulfate formation by

O_3 may occur on the surface of sea salt and dust aerosols. Aerosol surface area can impact the importance of these heterogeneous pathways. The lifetime of sulfate to loss via wet and dry deposition is about one week (Park et al., 2004). The $\Delta^{17}O(SO_4^{2-})$ value of sulfate formed by OH oxidation is ~ 0 ‰, O_3 is 6.25–8.75 ‰, H_2O_2 is ~ 0.65 ‰, and O_2 is −0.09 ‰. Sulfate formed by HOCl or HOBr has $\Delta^{17}O(SO_4^{2-})$ near 0 ‰, as the

reaction proceeds via hydrolysis, so the oxygen atom comes from a water molecule (Fogelman et al., 1989; Troy and Margerum, 1991).

2.2 Nitrate chemistry and $\Delta^{17}O$

Nitrogen oxides are emitted to or produced in the atmosphere via high-temperature processes including fossil fuel combustion, biomass burning, and lightning as well as

via soil microbes and the atmospheric oxidation of ammonia. Reaction of N_2O with $O(^1D)$ in the stratosphere produces NO_x that enters the polar troposphere either via gas-phase stratosphere-troposphere mixing or, after conversion to nitrate, via sedimentation of stratospheric aerosols (Salawitch et al., 1989). Finally, photolysis of snowpack nitrate releases NO_x to the polar boundary layer which may re-deposit locally or else-

where in Antarctica. Isotopic evidence suggests that nitrate at an East Antarctic coastal site is derived from snowpack NO_x emissions upslope on the East Antarctic plateau (Savarino et al., 2007). Antarctic boundary layer meteorology suggests that WAIS Di-

WAIS Divide sulfate and nitrate isotopes

E. D. Sofen et al.

Title Page

Abstract	Introduction
Conclusions	References
Tables	Figures

|◄ | ►|

◄ | ►

Back | Close

Full Screen / Esc

Printer-friendly Version

Interactive Discussion

vide is located in an area of low-level divergence of the katabatic winds and likely sees little transport across the Transantarctic Mountains from East Antarctica (Parish and Bromwich, 2007), suggesting that WAIS Divide is not strongly influenced by fluxes of NO_x and NO_3^- from East Antarctica. Recent trace gas observations combined with back-trajectory analysis at WAIS Divide find that during a three-week study period, 27 % of air masses came from the East Antarctic Plateau, with an additional 41 % contribution from lower-elevation (< 2500 m) East Antarctic locations. However, they find that the lifetime of NO_x and HNO_3 was short enough so that East Antarctica is not expected to be a major source of NO_x or nitrate to WAIS Divide (Masclin et al., 2013). The relative importance of these NO_x sources to nitrate deposited in West Antarctica is not well quantified (Wolff et al., 2008).

In sunlight (daytime or polar summer), NO_x cycles rapidly via oxidation of NO by O_3, RO_2, or BrO and photolysis of NO_2. Figure 1b illustrates the major nitrate formation pathways. NO_2 is oxidized in the daytime by OH to form HNO_3 or by BrO to $BrONO_2$. Formation of $BrONO_2$ is followed by hydrolysis to form HNO_3 on the surface of aerosols. At night, NO_2 is oxidized by O_3 to form the nitrate radical (NO_3), followed by conversion to HNO_3 via hydrogen abstraction of either DMS or hydrocarbons or by N_2O_5 hydrolysis on the surface of aerosols. During daytime, NO_3 is photolyzed back to NO_x, preventing significant daytime nitric acid production by these latter reactions. Once formed, aerosol thermodynamics determine the partitioning of nitric acid between the gas phase and aerosol phase. In the aerosol phase, HNO_3 may dissolve in water and dissociate into $H^+ + NO_3^-$. The oxygen isotopic compositions of HNO_3 and NO_3^- are indistinguishable, as gas-aerosol partitioning will only produce a mass-dependent fractionation. References to "nitrate" and $\Delta^{17}O(NO_3^-)$ refer to the sum of $HNO_3 + NO_3^-$ and its isotopic composition, unless otherwise specified. The global average lifetime of nitrate is 4–6 days and is lost from the atmosphere via dry and wet deposition to the surface (Xu and Penner, 2012).

The oxygen isotopic composition of nitrate ($\Delta^{17}O(NO_3^-)$) is determined by the isotopic composition of NO_2 ($\Delta^{17}O(NO_2)$) and the oxidation pathway of NO_2 to nitrate.

Full Screen / Esc

Printer-friendly Version

Interactive Discussion

The $\Delta^{17}O(NO_2)$ is determined by the relative abundance of O_3, RO_2, and BrO. For a given value of $\Delta^{17}O(NO_2)$, NO_2+OH produces the lowest $\Delta^{17}O(NO_3^-)$ value and NO_3+DMS/HC or $BrONO_2$ hydrolysis produce the highest $\Delta^{17}O(NO_3^-)$. Observations of $\Delta^{17}O(NO_3^-)$ from Antarctic aerosol range from 20–43.1 ‰ (Savarino et al., 2007). Postdepositional processing also impacts $\Delta^{17}O(NO_3^-)$. When snowpack NO_3^- is photolyzed, released to the boundary layer as NO_x, and oxidized back to NO_3^-, it acquires a $\Delta^{17}O$ reflecting oxidant abundances local to the sunlit Antarctic boundary layer.

2.3 Nitrate $\delta^{15}N$

The nitrogen isotopic composition of nitrate ($\delta^{15}N(NO_3^-)$) is thought to be mainly influenced by the source of NO_x and the extent of postdepositional loss of nitrate from the snowpack (Morin et al., 2009; Savarino et al., 2007). NO_x sources span a range of $\delta^{15}N(NO_x) = -49$ to $+25$ ‰ (Felix et al., 2012, and references therein), but are uncertain due in part to fractionation during NO_x collection (Fibiger and Hastings, 2012). Midlatitude aerosol measurements of $\delta^{15}N(NO_3^-)$ suggest a narrower range, with anthropogenically-influenced $\delta^{15}N(NO_3^-) = 0$–6 ‰, while nitrate from natural NO_x sources has $\delta^{15}N(NO_3^-) = -4 \pm 2$ ‰ (Morin et al., 2009).

Photolysis of nitrate in snowpack enriches snowpack $\delta^{15}N(NO_3^-)$ and is a source of low-$\delta^{15}N$ NO_x to the boundary layer (Blunier et al., 2005). The magnitude of the fractionation factor due to photolysis remains uncertain (Erbland et al., 2013), and the actual impact on snowpack $\delta^{15}N(NO_3^-)$ depends on the extent to which NO_x is exported from a site before redeposition. The amount of postdepositional loss, and therefore the extent of snowpack $\delta^{15}N(NO_3^-)$ enrichment, depends upon snow accumulation rate (Frey et al., 2009) and the concentration of UV absorbing impurities in the snow (Zatko et al., 2013). Low-accumulation East Antarctic Plateau sites have snowpack $\delta^{15}N(NO_3^-)$ up to 340 ‰ (Frey et al., 2009).

3   Methods

3.1   Description of the WAIS Divide site and cores

The West Antarctic Ice Sheet Divide (WAIS Divide) ice core site is located at 79.467° S, 112.085° W at a surface elevation of 1176 m. The site was selected due to its proximity 24 km downslope from the ice flow divide – providing good ice stratigraphy – and its annual accumulation rate of $0.22\,\mathrm{m\,a^{-1}}$ – comparable to Greenland summit ice cores. An accumulation rate comparable to that in Greenland allows for direct comparison of many ice core records between hemispheres. The high accumulation rate at the site also has the potential to mitigate the impact of postdepositional processes on many chemical species such as H_2O_2 and nitrate. In addition to a long core (WDC06A) that almost reaches the ice sheet bed, a number of short cores of $\sim 100\,\mathrm{m}$ were drilled to provide greater ice volume for studies of the recent past and development of new analytical techniques.

3.2   Ice core sampling

The upper 577 m of the WAIS Divide ice core, spanning the time period from 427 BCE to 2006 CE with a dating uncertainty of approximately ±2 % (McGwire et al., 2011), was sampled for measurement of the isotopic composition of sulfate and nitrate. Ice samples from the WAIS Divide ice cores were cut at the National Ice Core Lab (NICL; Denver, CO, USA). Each section consisted of a 3 cm × 3 cm cross section pieces, generally 1 m in length. Based upon concentration measurements, 1 m sections were combined to achieve sample sizes adequate for isotopic analysis. Low sulfate concentrations in the ice required the combination of 7–15 m of ice per isotopic analysis, corresponding to 27–68 yr of snow accumulation per sample.

Table 1 summarizes the sampling and isotopic measurement scheme. Sulfate isotope measurements were conducted on six samples from the WDC05A core between the surface and 69.80 m and were previously published (Kunasek et al., 2010). Nitrate

^{15}N was measured on 70 samples of approximately 1 m length from the surface to 69.80 m in the WDC05A core. Nitrate Δ^{17}O was measured at 1 m resolution on 121 samples between the surface and 129.196 m in the WDC05Q core. The 1 m resolution δ^{15}N(NO$_3^-$) and Δ^{17}O(NO$_3^-$) were measured on separate ice cores because the evaporation process used to concentrate the nitrate for Δ^{17}O(NO$_3^-$) analysis fractionated δ^{15}N(NO$_3^-$). Upon adoption of a new method of concentrating nitrate using an anion exchange resin following (Frey et al., 2009), all three sets of isotopes (Δ^{17}O(SO$_4^{2-}$), Δ^{17}O(NO$_3^-$), and δ^{15}N(NO$_3^-$)) were measured on thirty-two samples from the WDC06A core between 114 m and 577 m.

3.3 Isotopic analysis

3.3.1 Nitrate isotopes

After melting ice samples in a laminar flow clean hood, 500 mL aliquots were taken for nitrate isotope analysis. All Δ^{17}O(NO$_3^-$) measurements were conducted in triplicate, as was the δ^{15}N(NO$_3^-$) for the 32 samples from the WDC06A core. δ^{15}N(NO$_3^-$) was measured without replication at 1 m resolution in the upper 69.80 m on the WDC05A core. Nitrate converted to N$_2$O via bacterial denitrification and analyzed for δ^{15}N and Δ^{17}O following quantitative decomposition of N$_2$O into O$_2$+N$_2$ in a heated gold tube (Sigman et al., 2001; Kaiser et al., 2007).

Nitrate Δ^{17}O(NO$_3^-$) and δ^{15}N(NO$_3^-$) are measured relative to VSMOW and air N$_2$, respectively. Their values are corrected for nonlinearity associated with sample size based on replicate measurements of international (USGS-34: Δ^{17}O(NO$_3^-$) = −0.1 ‰ and δ^{15}N(NO$_3^-$) = 1.8 ‰; USGS-35; Δ^{17}O(NO$_3^-$) = 21.6 ‰ and δ^{15}N(NO$_3^-$) = 2.7 ‰) and in-house laboratory standards over a range of sizes. Uncertainty in the δ^{15}N(NO$_3^-$) from the WDC06A core and all Δ^{17}O(NO$_3^-$) measurements is the maximum of the standard deviation of the triplicate measurement due to inter-sample variability or un-

Title Page

Abstract | Introduction

Conclusions | References

Tables | Figures

|◄ | ►|

◄ | ►

Back | Close

Full Screen / Esc

Printer-friendly Version

Interactive Discussion

certainty in the yield correction. As replicates were not done on the 1 m resolution $\delta^{15}N(NO_3^-)$ (0–69.8 m), a fixed uncertainty of ±0.55 ‰ is used, based on the 1σ error in the repeated measurement of standards.

3.3.2 Sulfate isotopes

The rest of the melt water (approx. 6–14 L), intended for sulfate isotope analysis, was heated on a hot plate to 60 °C in a laminar flow hood to concentrate the sample by evaporation to approximately 50 mL volume. Sulfate was separated from other anions using a Dionex 2000 ion chromatograph with an IonPac AG15 column (4 × 50 mm) for anion preconcentration, IonPac AG19 guard column (4 × 50 mm), IonPac AS19 separation column (4 × 250 mm), ASRS-Ultra II suppressor (4 mm), and Dionex conductivity detector. The extracted sulfate (as H_2SO_4 solution) was frozen and shipped to UCSD where it was converted to Ag_2SO_4 using an Ag^+ exchange resin. The $\Delta^{17}O(SO_4^{2-})$ was measured at UCSD using the silver salt pyrolysis method described by Kunasek et al. (2010) and Savarino et al. (2001), except that sulfur isotopes were not measured beyond the upper 70 m as they proved difficult to interpret (Kunasek et al., 2010). Due to sample size requirements, only a single $\Delta^{17}O(SO_4^{2-})$ analysis was performed for each depth interval.

Sulfate $\Delta^{17}O$ is first corrected for isotopic exchange with quartz (Schauer et al., 2012) then for sea salt sulfate based on high resolution Na^+ measurements from continuous-flow analysis (performed at DRI) averaged to the resolution of the isotope measurements. We assume a sulfate to sodium ratio of $k = 0.25$ (Holland, 1978). An uncertainty in the $\Delta^{17}O(SO_4^{2-})$ measurements of ±0.3 ‰ is determined from the 1σ error in the repeated measurement of standards.

3.4 Box model description

To interpret the observations of $\Delta^{17}O(SO_4^{2-})$ and $\Delta^{17}O(NO_3^-)$ to changes in mid-to-high latitude Southern Hemisphere oxidant abundances, we developed a Monte Carlo

modeling framework for box models of the production and isotopic composition sulfate and nitrate.

3.4.1 Model design

The nitrate box model chemistry was previously described by Kunasek et al. (2008). The sulfate box model chemistry scheme is the same as that used in sulfate isotope simulations in the GEOS-Chem (http://www.geos-chem.org) global three-dimensional chemical transport model (Alexander et al., 2012). Both box models calculate monthly mean production rates for each pathway described in Sects. 2.1 and 2.2 and shown in Fig. 1. The sulfate model goes a step further to calculate concentrations based on the global mean lifetime for each form of sulfate (gas-phase, aqueous, or heterogeneous) based on a global sulfate aerosol simulation (Alexander et al., 2009). This step is not necessary for nitrate, because the thermodynamic partitioning of nitrate between gas and aerosol phases means that the lifetime of nitrate is independent of its production mechanism. The nitrate model first calculates the steady-state NO_2 production by O_3 and RO_2 followed by the oxidation of NO_2 to NO_3^-. The models calculate monthly mean production rates (nitrate) and concentrations (sulfate) associated with each formation mechanism. The monthly and annual average oxygen isotopic compositions of sulfate and nitrate are then calculated based on the oxidant isotopic composition and isotopic transfer associated with each pathway (and the steady-state ratio of production by O_3 and RO_2 for NO_x cycling). Halogen chemistry is included in both models as a sensitivity study. In the nitrate model, we include $NO_2 + BrO$ and the hydrolysis of $BrONO_2$ on aerosols as in Kunasek et al. (2008). In the sulfate model, we include aqueous-phase sulfate production by both HOBr and HOCl using assumed and measured (for SO_3^{2-}) reaction rate constants (Fogelman et al., 1989; Troy and Margerum, 1991).

3.4.2 Model boundary conditions

Box model boundary conditions are generally taken from a GEOS-Chem simulation of the year 2005 for the geographical region of interest (Southern Ocean and South American boundary layers for sulfate and nitrate, respectively). For the nitrate model, the fraction of the month in daylight is calculated based on latitude (50° S).

Sulfate model boundary conditions include concentrations of SO_2, HNO_3, O_3, OH, H_2O_2, dust (in four size bins: 0.1–1.0, 1.0–1.8, 1.8–3.0, 3.0–6.0 μm), and sea salt (in two size bins 0.1–0.5, 0.5–10 μm). Physical parameters include air density, temperature, specific humidity, and surface pressure. For aqueous phase chemistry, cloud water pH is varied between 4.5 and 6.0 to span the pH range across which aqueous sulfate formation and $\Delta^{17}O(SO_4^{2-})$ are highly sensitive to pH. Observations of cloud water pH in clean marine environments span a range of 3.8–6.1 (Faloona, 2009, and references therein). We neglect consideration of pH < 4.5 because it is unlikely to occur over the remote Southern Ocean and these acidic conditions are unlikely to produce sulfate with a $\Delta^{17}O$ consistent with observations, as sulfate formation by O_3 will be suppressed. Cloud liquid water content is taken from GEOS-Chem, where it is calculated based on temperature, and cloud fraction from GEOS-Chem is scaled to Southern Ocean low cloud fraction observations (Eastman et al., 2011) while retaining its calculated vertical structure.

Nitrate model boundary conditions include concentrations of NO, NO_2, HO_2, O_3, OH, NO_3, VOCs (acetaldehyded, $\geq C_4$ alkanes, $> C_2$ aldhydes), DMS, and N_2O_5, as well as the photolysis rate of NO_2, NO_2 production rates by RO_2 and O_3, and aerosol surface area from GEOS-Chem. Physical parameters include air temperature and air density. When BrO is included, we assume a fixed concentration of 1 pmol mol^{-1}.

3.4.3 Monte Carlo approach

The mean and standard deviation (σ_{ox}) of each monthly oxidant concentration is calculated based on the spatial variability across the region of interest (Southern Ocean

Title Page

Abstract | Introduction

Conclusions | References

Tables | Figures

◄ | ►

◄ | ►

Back | Close

Full Screen / Esc

Printer-friendly Version

Interactive Discussion

for $\Delta^{17}O(SO_4^{2-})$; extratropical South America for $\Delta^{17}O(NO_3^-)$) in a present-day simulation using the GEOS-Chem global chemical transport model. To span a large range of oxidant conditions, monthly mean concentrations of each oxidant are independently varied over $3\sigma_{ox}$ to produce a wide Gaussian distribution of possible oxidant conditions (preserving the seasonal cycle), while all other boundary conditions are held constant (Sect. 5.4 justifies these assumption that other boundary conditions are held constant). The distributions of oxidant concentrations are then repeatedly sampled and the box model is run using these boundary conditions and the annual $\Delta^{17}O(SO_4^{2-})$ or $\Delta^{17}O(NO_3^-)$ is calculated. We then search for pairs of simulations that match the observed change in $\Delta^{17}O$. These pairs of simulations that match the $\Delta^{17}O$ observations provide the corresponding changes in annual mean oxidant concentrations required to match the ice core observations.

3.4.4 Model limitations

There is uncertainty in the assumed $\Delta^{17}O$ of oxidants, the isotopic transfer from oxidants to products, and the chemical mechanisms in the box models, all of which could bias the calculation of $\Delta^{17}O(NO_3^-)$ or $\Delta^{17}O(SO_4^{2-})$ and concentrations in any given time period. Therefore, we focus on the magnitude of the change in $\Delta^{17}O$ between time periods of interest, since the potential biases in the isotopic assumptions will be similar for each time period. Identical assumptions about the $\Delta^{17}O$ values of the oxidants, their isotopic transfer, and the chemistry responsible for sulfate and nitrate formation in a global model produce good agreement with a global compilation of $\Delta^{17}O(SO_4^{2-})$ and $\Delta^{17}O(NO_3^-)$ observations in the present-day (Alexander et al., 2009, 2012).

The above box model approach does not include coupling between oxidants as if they are in a photochemical box model. However, a photochemical box model will not provide an accurate representation of the relationships between oxidants on the time or spatial scales of interest because of the stiffness of the system as determined by the large difference in lifetimes between OH and O_3 (Seinfeld and Pandis, 2006). Fur-

thermore, the model does not allow for the mixing of sulfate or nitrate from multiple regions/sources that is likely representative of samples from WAIS Divide. While a global model would provide this, it would be less flexible for exploring how chemistry changes impact $\Delta^{17}O$.

4 WAIS divide ice core observations

Figure 2 shows the WAIS Divide ice core measurements of $\Delta^{17}O(SO_4^{2-})$, $\Delta^{17}O(NO_3^-)$, and $\delta^{15}N(NO_3^-)$. This record represents the first ice core record of $\Delta^{17}O(NO_3^-)$ and $\Delta^{17}O(SO_4^{2-})$ sampled continuously over the past 2400 yr.

$\Delta^{17}O(SO_4^{2-})$ is sampled at 7–15 m (27–68 yr) resolution and varies between 1.8 ‰ and 3.7 ‰ over the entire record (Table 1 summarizes the sampling and isotopic measurement scheme). Prior to 1810 CE, $\Delta^{17}O(SO_4^{2-})$ is less than 2.8 ‰. From 1810–2005 CE, $\Delta^{17}O(SO_4^{2-})$ is greater than 3 ‰, with a maximum of 3.7 ‰ between 1837 and 1880 CE. There is a 1.1 ‰ difference in the mean $\Delta^{17}O(SO_4^{2-})$ between the period prior to 1810 and that after 1837. The 1810–1837 sample is excluded from this analysis because it is strongly influenced by the 1810 and Tambora volcanic eruptions (Kunasek et al., 2010). At the same time as the increase in $\Delta^{17}O(SO_4^{2-})$, there is a decrease in [MSA] and a slight, but not statistically significant, decrease in the [MSA]/[nssSO$_4^{2-}$] ratio (Fig. 3). This is suggestive of a change in the chemistry of DMS oxidation at the same time as the observed change in the chemistry of SO$_2$ oxidation.

$\Delta^{17}O(NO_3^-)$ is sampled at 1 m (1.8–4.8 yr) resolution in the upper part of the core (0–129 m depth, spanning 1521–2000 CE) and varies between 21.4 ‰ and 43.7 ‰. Figure 4 includes an expanded version of the 1 m resolution data from Fig. 2. Large intersample variability in the high-resolution $\Delta^{17}O(NO_3^-)$ record highlights its local nature, in that it represents the signal of NO$_x$ cycling and nitrate formation in the NO$_x$ source regions. Prior to 1586 CE, $\Delta^{17}O(NO_3^-)$ and $\delta^{15}N(NO_3^-)$ are sampled at the same res-

olution as $\Delta^{17}O(SO_4^{2-})$. For the consideration of long-term trends and comparison to $\Delta^{17}O(SO_4^{2-})$, the 1 m resolution $\Delta^{17}O(NO_3^-)$ and $\delta^{15}N(NO_3^-)$ records are smoothed by calculating a concentration-weighted average of the 1 m resolution nitrate isotope data to the temporal resolution of the $\Delta^{17}O(SO_4^{2-})$ measurements. Considering these low-resolution $\Delta^{17}O(NO_3^-)$ data, the maximum $\Delta^{17}O(NO_3^-)$ of 37.8 ‰ occurs between 802 and 865 CE. The minimum of 26.7 ‰ occurs between 1977 and 2006 CE.

The ice core $\delta^{15}N(NO_3^-)$ at 1 m resolution (0–69.8 m; 1774–2005 CE) varies between 1.0 ‰ (1787–1791 CE) and 15.7 ‰ (1961–1964 CE and 1998–2000 CE). The low-resolution $\delta^{15}N(NO_3^-)$ varies between 1.5 ‰ (316–370 CE) and 9.9 ‰ (1422–1481 CE), with a gradual upward trend since 370 CE. WAIS Divide $\delta^{15}N(NO_3^-)$ does not exhibit the large enrichments observed in East Antarctic sites and are similar in range to $\delta^{15}N(NO_3^-)$ from Greenland summit ice cores (−15.3–16.7 ‰) (Hastings, 2010). The similarity to Greenland is likely due to comparable snow accumulation rates (22–25 cm yr^{-1} Fegyveresi et al., 2011) that limit the degree of postdepositional processing.

While there is significant variability in the low resolution $\Delta^{17}O$ data in the early part of the ice core record, the largest changes in both $\Delta^{17}O(NO_3^-)$ and $\Delta^{17}O(SO_4^{2-})$ occur in the period after 1800 CE. The maximum $\Delta^{17}O(SO_4^{2-})$ occurs in the sample spanning 1837–1880 CE with slightly lower values in the more recent samples, but the entire period 1837–2008 has a higher $\Delta^{17}O(SO_4^{2-})$ than any earlier sample and the post-1837 samples are indistinguishable from each other within the laboratory precision (±0.3 ‰). In contrast to the step increase in $\Delta^{17}O(SO_4^{2-})$, $\Delta^{17}O(NO_3^-)$ gradually declines throughout the past 1000 yr, with a more rapid decline beginning in the 1860s. While there is short term variability in the 1 m resolution $\Delta^{17}O(NO_3^-)$ record in the 1500s that is comparable in magnitude to the recent decline in $\Delta^{17}O(NO_3^-)$, on the 100 to 200 yr timescale, the downward trend in $\Delta^{17}O(NO_3^-)$ between ∼ 1863–2000 CE is statistically distinct from any other centennial trends in the 1 m resolution record (1521–2000 CE). Trends for all 100 yr intervals with starting dates of 1521–1859 CE have a mean slope of −0.5±2.3 ‰ century^{-1}, while those trends starting after 1863 CE have

a mean slope of -6.7 ± 0.8‰ century^{-1}. Similarly, the decrease in $\Delta^{17}O(NO_3^-)$ when averaged to the resolution of the $\Delta^{17}O(SO_4^{2-})$ data is -5.6‰ from 1878–2000 CE.

Finally, there is a downward excursion in $\Delta^{17}O(SO_4^{2-})$, $\Delta^{17}O(NO_3^-)$, and $\delta^{15}N(NO_3^-)$ around the year 360 CE. The magnitude of the excursion in $\Delta^{17}O(NO_3^-)$ is comparable in magnitude to the changes observed between the 1860s and present-day. There is no evidence of contamination in these samples and the deviation in both $\Delta^{17}O(NO_3^-)$ and $\delta^{15}N(NO_3^-)$ spans multiple samples. However, no other chemical tracers from the WAIS Divide ice core show a similar excursion. At this time, we do not attempt to explain the observed isotopic deviation around 360 CE and instead focus on the sustained changes in $\Delta^{17}O(SO_4^{2-})$ and $\Delta^{17}O(NO_3^-)$ between 1800 CE and the present.

5 Comparison of $\Delta^{17}O$ to other ice core records

To try to constrain the interpretation of the observed $\Delta^{17}O$ changes, we compare the sulfate and nitrate isotopes to other ice core measurements from WAIS Divide that are related to sulfate and nitrate formation (Figs. 4 and 3). These measurements are made using continuous-flow analysis, providing cm-scale resolution, which are averaged to the resolution of the isotope records presented here. Records that come from the same core as the isotope record of interest are averaged with respect to depth. For comparison of measurements between different cores, high-resolution data is divided into segments to match the resolution of the isotope data in the time domain and then averaged based on depth.

We calculate correlation coefficients and determine their statistical significance using the p value (≤ 0.05) with the number of degrees of freedom adjusted based upon the autocorrelation in the time series (Bretherton et al., 1999).

5.1 $\Delta^{17}O(SO_4^{2-})$ comparison

Measurements of ice core acidity (Fig. 3) or calculated $[H^+]$ based on sulfate, nitrate, and ammonium concentrations provide the best available insight into possible changes in cloud water pH, which impacts S(IV) speciation and the relative importance

5 of oxidation by O_3 and H_2O_2. However, the acidity record shows little variability, and $\Delta^{17}O(SO_4^{2-})$ does not correlate with either ice core acidity or $[H^+]$, making it unlikely that a change in cloud water pH could explain the observed change in $\Delta^{17}O(SO_4^{2-})$.

Similarly, $\Delta^{17}O(SO_4^{2-})$ shows no correlation with concentrations of transition metals (Fe or Mn) (Fig. 3) that may impact the aqueous-phase oxidation of S(IV) by O_2.

10 Furthermore, CTM studies indicate that metal-catalyzed oxidation of S(IV) is a minor sulfate production pathway in the extratropical Southern Hemisphere (Alexander et al., 2009; Sofen et al., 2011). The lack of a relationship between $\Delta^{17}O(SO_4^{2-})$ and transition metal concentrations or acidity is notable, as it has been demonstrated that metal-catalyzed oxidation of S(IV) by O_2 is important for describing the observed variability

15 of $\Delta^{17}O(SO_4^{2-})$ in a Greenland ice core over the same time period (Sofen et al., 2011).

$\Delta^{17}O(SO_4^{2-})$ does not show a statistically significant correlation with $[Na^+]$, a proxy for sea salt (Fig. 3). Sea-salt sulfate represents 15–22 % of total sulfate in these samples. However, $[Na^+]$ does not change in the early-1800s in a similar way to $\Delta^{17}O(SO_4^{2-})$. The step-change in $\Delta^{17}O(SO_4^{2-})$ is present in the record prior to correction for sea salt

20 sulfate.

$\Delta^{17}O(SO_4^{2-})$ and sulfur concentrations (Fig. 3) are not correlated. This suggests that variability in $\Delta^{17}O(SO_4^{2-})$ is not controlled by changes in the magnitude of the sulfur source or the sulfur source region, as a change in the source region that impacted sulfate formation would likely be accompanied by a change in the amount of sulfate

25 transported to WAIS Divide.

Hydrogen peroxide is the one oxidant species that can be directly measured in ice cores. Oxidation of S(IV) by H_2O_2 is thought to be the dominant sulfate formation path-

way globally. Since $\Delta^{17}O(SO_4^{2-})$ of sulfate formed by H_2O_2 is only 0.65 ‰, an increase in $[H_2O_2]$ in the southern high latitudes should decrease $\Delta^{17}O(SO_4^{2-})$ at WAIS Divide. We find that the WAIS Divide $\Delta^{17}O(SO_4^{2-})$ and $[H_2O_2]$ records (Fig. 3) are not correlated. Ice core $[H_2O_2]$ does not significantly change during the early 19th c. when $\Delta^{17}O(SO_4^{2-})$ undergoes a step increase. However, H_2O_2 increases by $\sim 60\%$ in the period after 1837 CE, when $\Delta^{17}O(SO_4^{2-})$ remains relatively constant.

There is no available ice core proxy for fractional cloud cover or cloud liquid water content, both of which impact sulfate formation and thus $\Delta^{17}O(SO_4^{2-})$. We assume no change in these parameters based on the fact that climate has been relatively stable over this time period, as indicated by temperature proxies (e.g. $\delta^{18}O(H_2O)$).

5.2 $\Delta^{17}O(NO_3^-)$ comparison

Due to the fact that H_2O_2 forms via the self-reaction of HO_2, we would expect the large-scale increase in H_2O_2 to be reflected in a decrease in $\Delta^{17}O(NO_3^-)$ due to the increased importance of HO_2 in NO_x cycling as long as the relative increase in $[HO_2]$ is greater than the increase in $[O_3]$. We would expect a larger change in $\Delta^{17}O(NO_3^-)$ than H_2O_2 if organic peroxides were also increasing, since H_2O_2 may not be influenced as strongly by changes in organic peroxide concentration $[RO_2]$ as it is by HO_2. However, this may be alleviated by a simultaneous increase in $[O_3]$, since $\Delta^{17}O(NO_3^-)$ reflects $[O_3]/[RO_2]$. If $\Delta^{17}O(NO_3^-)$ is influenced by local Antarctic boundary layer chemistry, we expect $\Delta^{17}O(NO_3^-)$ to decrease at a more rapid rate beginning in the 1970s due to the impacts of the recent increase in UV flux on H_2O_2 (Lamarque et al., 2011).

Indeed, $[H_2O_2]$ (Fig. 4) is anti-correlated with the 1 m resolution $\Delta^{17}O(NO_3^-)$ between 1521–2000 CE ($R = -0.36$), consistent with an increase in the importance of RO_2 in NO_x cycling. The temporal resolution in $\Delta^{17}O(NO_3^-)$ observations is not high enough to test whether the ozone hole impacts $\Delta^{17}O(NO_3^-)$ through snowpack photodenitrification or the oxidizing capacity of the Antarctic boundary layer. The trend in

$\Delta^{17}O(NO_3^-)$ over the last thirty years ($-4 \pm 4\,‰\,century^{-1}$) is indistinguishable from that of last 100 yr ($-5 \pm 1\,‰\,century^{-1}$), further suggesting that postdepositional loss does not have a strong influence on ice core nitrate or its isotopes at WAIS Divide.

Ice core observations of [MSA] (Fig. 3), indicative of DMS emissions, show a downward trend over the past 1800 yr, but the correlation with the low-resolution $\Delta^{17}O(NO_3^-)$ is not significant. A reduction in DMS would diminish the fraction of nitrate formed through the hydrogen abstraction pathway, reducing the $\Delta^{17}O(NO_3^-)$. Therefore, the trend in MSA is consistent with the long-term trend in $\Delta^{17}O(NO_3^-)$. However, there are a number of complicating factors in the interpretation of the MSA record. First, it assumes a constant relationship between DMS and MSA concentrations in the atmosphere, which could vary with changing oxidants. Second, MSA is also sensitive to postdepositional loss from the snowpack through volatilization (Weller et al., 2004), and the downward trend in MSA is consistent with increasing postdepositional processing as accumulation declines (as is the case for $\Delta^{17}O(NO_3^-)$ and $\delta^{15}N(NO_3^-)$), although it has been argued that postdepositional loss of MSA is insignificant when snow accumulation is higher than $0.1\,m\,yr^{-1}$ water equivalent (Weller et al., 2004). Finally, the past 150 yr in the MSA record do not show a change in [MSA] akin to that observed in $\Delta^{17}O(NO_3^-)$ (Fig. 4) and the two records are not significantly correlated over this time period (using 1 m resolution measurements).

The $\Delta^{17}O(NO_3^-)$ is not correlated with nitrate concentrations (Fig. 4) at 1 m resolution between 1521 CE and present, and there is little trend in the concentration of nitrate over the past 200 yr. This, in conjunction with the absence of large changes in [NO$_3^-$] or $\delta^{15}N(NO_3^-)$ all suggest that sources of nitrate to WAIS Divide have likely remained constant over this period, as a major shift in source regions would likely be accompanied by a change in the amount of nitrate transported to WAIS Divide and possibly the isotopic composition.

In addition to nitrate that forms at lower latitudes, NO_x emitted in midlatitude continental regions could be transported to Antarctica via the reservoir molecule perox-

yacetyl nitrate (PAN), which then thermally decomposes, releasing NO_x, which will then be oxidized to NO_3^- in the local Antarctic atmosphere. While there is no proxy for PAN, mean PAN concentration of $13 \pm 7\,\text{pmol}\,\text{mol}^{-1}$ with a slow decomposition rate of $0.05\,\text{pmol}\,\text{mol}^{-1}\,\text{h}^{-1}$ are found at Neumayer (Jacobi et al., 2000). More recent measurements at Neumayer suggest that PAN varies between a net sink (spring) and a net source (summer) of NO_x with PAN loss rates of between 0.17 and $0.58\,\text{pmol}\,\text{mol}^{-1}\,\text{h}^{-1}$ (Jones et al., 2011). PAN concentrations and loss rates are an order of magnitude lower than in the Arctic (Beine and Krognes, 2000), suggesting that PAN decomposition is an unimportant factor in WAIS Divide nitrate formation. Furthermore, while atmospheric PAN concentrations can be higher than inorganic nitrogen species during winter, snowpack nitrate concentrations correlate with inorganic reactive nitrogen (Jones et al., 2011), likely due to the longer lifetime to deposition of organic nitrate than inorganic nitrate (Wolff et al., 2008).

Finally, stratospheric denitrification is a potential source of high-$\Delta^{17}O$ nitrate to Antarctica, although its magnitude in West Antarctica is unknown. While it may impact the magnitude of the average $\Delta^{17}O(NO_3^-)$ observed in the WAIS Divide ice core, there is no reason to expect systematic changes in the polar stratospheric nitrate flux prior to the formation of the ozone hole in the 1970s. Furthermore, the lower elevation of West Antarctica likely means that stratospheric deposition is less important than on the East Antarctic Plateau.

5.3   Influence of postdepositional processing on $\Delta^{17}O(NO_3^-)$

The magnitude of nitrate postdepositional processing impacts the extent to which $\Delta^{17}O(NO_3^-)$ reflects regional oxidants from where the NO_3^- is originally formed vs. local oxidants from snowpack NO_x being oxidized back to NO_3^- in the Antarctic boundary layer. The 2400 yr $\delta^{15}N(NO_3^-)$ record is negatively correlated with snow accumulation rate (Fegyveresi et al., 2011) ($R = -0.62$) and positively correlated with $[NO_3^-]$ ($R = 0.58$; Fig. 3). Similarly, at low resolution, $\delta^{18}O(H_2O)$ (Fig. 3), a temperature proxy,

is anticorrelated with $\delta^{15}N(NO_3^-)$ ($R = -0.63$) over the entire 2400 yr record. However, $\Delta^{17}O(NO_3^-)$ and $\delta^{15}N(NO_3^-)$ are not correlated with each other. The correlations between $\delta^{15}N(NO_3^-)$, $[NO_3^-]$, snow accumulation, and temperature suggests that on long timescales some degree of postdepositional processing of snowpack NO_3^- is occurring at WAIS Divide. Increasing postdepositional processing due to the long-term decline in snow accumulation over the past ~ 2000 yr is likely responsible for the gradual downward trend in $\Delta^{17}O(NO_3^-)$ and upward trend in $\delta^{15}N(NO_3^-)$. However, the magnitude of the $\delta^{15}N(NO_3^-)$ values (1.0–15.7‰) is comparable to Greenland snowpack nitrate (Hastings et al., 2004, 2009) and only slightly enriched compared to NO_x emissions and mid-latitude aerosol observations (Morin et al., 2009; Felix et al., 2012), suggesting that the majority of nitrate is well-preserved in the snowpack. This is in contrast to East Antarctica where snowpack $\delta^{15}N(NO_3^-)$ enrichments on the order of 300‰ are observed. A flux of NO_x emitted from East Antarctic snowpack and transported to WAIS Divide could also contribute to the low $\delta^{15}N(NO_3^-)$ values observed at WAIS Divide, but the similarity in $\delta^{15}N(NO_3^-)$ at WAIS Divide and Greenland summit sites with comparable snow accumulation rate suggest that this is not the case. Furthermore, while the 1 m resolution $\delta^{15}N(NO_3^-)$ between 1774–2008 CE is anticorrelated with the snow accumulation rate (Fig. 4; $R = -0.35$), the 1 m resolution $\Delta^{17}O(NO_3^-)$ is not correlated with snow accumulation, $[NO_3^-]$, or $\delta^{15}N(NO_3^-)$ over the period 1521–2000 CE, suggesting that postdepositional processing does not have a controlling influence on higher frequency variability, such as the downward trend in $\Delta^{17}O(NO_3^-)$ since the 1860s.

5.4 Non-oxidant influences on $\Delta^{17}O$

The above comparisons between sulfate and nitrate isotopes and other tracers from the WAIS Divide ice cores include several related to the non-oxidant influences on $\Delta^{17}O$. These measurements include ice core acidity (proxy for cloud water pH) (Pasteris et al., 2012), [Mn] and [Fe] (impacting metal-catalyzed S(IV) oxidation by O_2), [Na$^+$] (proxy

for sea salt), [MSA] (a proxy for DMS), [S] and [SO_4^{2-}] (proxy for sulfate sources), [NO_3^-] (proxy for nitrate sources), snow accumulation rate (related to postdepositional loss of nitrate), and $\delta^{18}O(H_2O)$ (temperature proxy). We find that most of these records either show no significant correlation with either nitrate or sulfate isotopes or are correlated only on long timescales (the entire 2400 yr record) with the low-resolution isotopes. While non-oxidant factors may contribute to the long term variability in the WAIS Divide sulfate and nitrate isotopes, visually and statistically, none of the records representing non-oxidant factors exhibit changes similar to the observed changes in $\Delta^{17}O(NO_3^-)$ and $\Delta^{17}O(SO_4^{2-})$ over the past 200 yr. This analysis suggests that variability in oxidant concentrations is the only possible explanation for the observed 1.1 ‰ increase in $\Delta^{17}O(SO_4^{2-})$ in the early 19th century and the 5.6 ‰ decrease in $\Delta^{17}O(NO_3^-)$ since the mid-19th century.

6 Monte Carlo box models of oxidant influences on $\Delta^{17}O$

To consider what changes in oxidants could cause the observed changes in $\Delta^{17}O$ since 1800 CE, we employ Monte Carlo box model simulations of sulfate and nitrate chemistry to investigate the magnitude of the oxidant changes implied in two time periods: the observed 1.1 ‰ increase in $\Delta^{17}O(SO_4^{2-})$ in the early 19th c. and 5.6 ‰ decrease in $\Delta^{17}O(NO_3^-)$ between the 1860s and present-day. Based on the evidence of little postdepositional processing at WAIS Divide, NO_x emissions and nitrate formation likely occur over Southern Hemisphere extratropical continental regions. The model uses boundary conditions from the extratropical South American boundary layer to calculate nitrate formation. The sulfate box model uses boundary conditions from the Southern Ocean marine boundary layer (MBL), reflecting the dominant source region for Antarctic sulfate (Patris et al., 2000; Cosme et al., 2005; Sofen et al., 2011).

6.1 Model $\Delta^{17}O$-oxidant sensitivity

The box models are first used to assess the sensitivity of $\Delta^{17}O(SO_4^{2-})$ and $\Delta^{17}O(NO_3^-)$ to changes in the concentration of each oxidant. Figure 5 shows the sensitivity of $\Delta^{17}O(SO_4^{2-})$ and $\Delta^{17}O(NO_3^-)$ to a relative change in the concentration of each oxidant normalized to the mean conditions extracted from GEOS-Chem for the boundary conditions described above (Southern Ocean and South American boundary layers, respectively) (Sofen et al., 2011). The slope of each curve represents the response of $\Delta^{17}O$ to a change in a particular oxidant.

$\Delta^{17}O(SO_4^{2-})$ is sensitive to changes in O_3, OH, and H_2O_2 over the Southern Ocean, with $\Delta^{17}O(SO_4^{2-})$ increasing (decreasing) with increasing O_3 (OH), and $\Delta^{17}O(SO_4^{2-})$ increasing with decreasing H_2O_2. $\Delta^{17}O(SO_4^{2-})$ becomes insensitive to changes in H_2O_2 at H_2O_2 concentrations greater than or equal to those of the present-day Southern Ocean marine boundary layer. The sensitivity of $\Delta^{17}O(SO_4^{2-})$ to H_2O_2 and O_3, as measured by the slope in Fig. 5, varies with their abundances, with higher sensitivity at lower $[H_2O_2]$ and $[O_3]$, respectively. The sensitivity of $\Delta^{17}O(SO_4^{2-})$ to [OH] is nearly linear over the range of OH concentrations considered.

$\Delta^{17}O(NO_3^-)$ is most sensitive to O_3 and RO_2, because $\frac{2}{3}$ of the $\Delta^{17}O$ of nitrate is determined during the NO_x-cycling step. $\Delta^{17}O(NO_3^-)$ increases (decreases) with increasing O_3 (RO_2). Changes in $\Delta^{17}O(NO_3^-)$ mainly reflect changes in $[O_3]/[RO_2]$; that is, the variability in $\Delta^{17}O(NO_3^-)$ is dominated by the NO_x-cycling step. $\Delta^{17}O(NO_3^-)$ only weakly depends on [OH] because NO_2+OH is always the dominant nitrate formation pathway during daytime. Including BrO in NO_x-cycling and the oxidation of NO_2 to NO_3^- via the hydrolysis of $BrONO_2$ changes the sensitivity of $\Delta^{17}O(NO_3^-)$ to each of the oxidants (dashed lines; Fig. 5). BrO oxidation of NO leads to an overall upward shift in $\Delta^{17}O(NO_3^-)$, as well as increasing the sensitivity of $\Delta^{17}O(NO_3^-)$ to changes in OH concentrations by providing a competing daytime NO_2-oxidation pathway.

Title Page

Abstract | Introduction

Conclusions | References

Tables | Figures

◄ | ►

◄ | ►

Back | Close

Full Screen / Esc

Printer-friendly Version

Interactive Discussion

These initial model results provide a qualitative explanation for how the change in $\Delta^{17}O(SO_4^{2-})$ and $\Delta^{17}O(NO_3^-)$ can have opposite signs between 1800 CE and the present given likely increases in both O_3 and H_2O_2 (and therefore RO_2), and a small decrease in OH in the extratropical Southern Hemisphere. In sum, the increase in $\Delta^{17}O(SO_4^{2-})$ and decrease in $\Delta^{17}O(NO_3^-)$ can be explained by an increase in the $[O_3]/[OH]$ ratio over the Southern Ocean and a decrease in the $[O_3]/[RO_2]$ ratio over Southern Hemisphere extratropical continents respectively, which is qualitatively consistent with our expectations.

6.2 Oxidant changes suggested by $\Delta^{17}O(NO_3^-)$

The nitrate Monte Carlo box model simulations indicate that to match the observed decrease in $\Delta^{17}O(NO_3^-)$, assuming no change ($\leq 5\%$) in Southern Hemisphere extratropical [OH] between the 1860s and 2000 CE, the $[O_3]/[RO_2]$ ratio must decrease by 48–84 % in the NO_3^- formation region. As shown in Fig. 6b, $[O_3]$ can increase by up to 110 % and $[RO_2]$ must increase by 100–350 % to be consistent with the $\Delta^{17}O(NO_3^-)$ observations. If [OH] decreases by 33 % (the lower bound of CTM studies), $[O_3]/[RO_2]$ must decrease by an even larger amount (−51 to −91 %). An increase in $[O_3]/[RO_2]$ is only possible if [OH] increases by > 250 %, which is highly unlikely over this time period due to increasing CH_4, which is a major sink of OH. If we assume a 25–63 % increase in $[O_3]$ since the preindustrial period based on global models (100 % based on southern extratropical Schönbein measurements) and no change in [OH], this implies a local 140–300 % (350 %) increase in $[RO_2]$ in high-latitude Southern Hemisphere NO_x source regions. CTM studies of preindustrial oxidant chemistry generally do not report changes in HO_2 or RO_2 species. If future model studies report changes in RO_2 in addition to O_3, they can use these ice core observations of $\Delta^{17}O(NO_3^-)$ as an additional constraint on paleo-oxidant modeling.

Title Page

Abstract | Introduction

Conclusions | References

Tables | Figures

◄ | ►

◄ | ►

Back | Close

Full Screen / Esc

Printer-friendly Version

Interactive Discussion

6.3 Oxidant changes suggested by $\Delta^{17}O(SO_4^{2-})$

Monte Carlo box model simulations are used to find changes in oxidant abundances that reproduce the observed 1.1 ‰ increase in $\Delta^{17}O(SO_4^{2-})$ in the early 19th c. Further constraints are imposed that $[H_2O_2]$ does not change, as ice core observations indicate that H_2O_2 does not begin to increase until the late 19th c., and $[O_3]$ cannot decrease. To match the observed increase in ice core $\Delta^{17}O(SO_4^{2-})$, the fractional increase in the $[O_3]/[OH]$ ratio in the Southern Ocean MBL must be at least 210 %, corresponding to a 12–18 % increase in the fraction of sulfate formed by O_3 in the aqueous phase. As shown in Fig. 6a, there is a near-linear relation between the required fractional changes in $[OH]$ (−40 to −80 %) and $[O_3]$ (0 to +120 %); simulations that match the observed $\Delta^{17}O(SO_4^{2-})$ change due to a large increase in $[O_3]$ correspond to a small decrease in $[OH]$. The minimum $[OH]$ decrease (−40 %), which is a much larger decrease than calculated by global models (−33 % to +14 %), corresponds to a 16 nmol mol^{-1} (120 %) increase in $[O_3]$. This fractional change in $[O_3]$ is greater than the global average change since the preindustrial period in most global models and is comparable in magnitude to that based on the Schönbein $[O_3]$ observations in the Southern Hemisphere extratropics. A global model sensitivity study suggests that a doubling in $[CH_4]$, which is much greater than the observed $[CH_4]$ increase in the early-1800s, leads to only a 26 % increase in $[O_3]/[OH]$ and changes in $[OH]$ and $[O_3]$ individually of ≤ 15 % in the Southern Hemisphere extratropics (Fig. A1; see Appendix A). Overall, the early timing and large magnitude of the oxidant changes required to explain the observed $\Delta^{17}O(SO_4^{2-})$ seem highly implausible. This, combined with the fact that ice core observations suggest no significant influence of the non-oxidant factors on sulfate formation, suggests that the change in $\Delta^{17}O(SO_4^{2-})$ may be due to changes in oxidants not considered in the box model analysis. In particular, this analysis points to a decreasing importance of another low-$\Delta^{17}O(SO_4^{2-})$-producing oxidant on this timescale. This is discussed further in Sect. 6.4.

The negligible changes in $\Delta^{17}O(SO_4^{2-})$ from 1837–2005 CE were previously shown to be consistent with the increases in extratropical Southern Hemisphere $[O_3]$ (25 to 27 %) and $[H_2O_2]$ (45 to 51 %), and a decrease in $[OH]$ (−15 %) in a CTM between the preindustrial and present-day mainly due to the offsetting effects of increasing $[O_3]$ and $[H_2O_2]$ on $\Delta^{17}O(SO_4^{2-})$ (Kunasek et al., 2010; Sofen et al., 2011). Monte Carlo model results for the time period 1837–2005 CE, when $\Delta^{17}O(SO_4^{2-})$ is constant and $[H_2O_2]$ increases 40–50 %, are consistent with the oxidant changes mentioned above. However, uncertainties in cloud water pH and $\Delta^{17}O(O_3)$ leads to a wide range in $[O_3]$ and $[OH]$ changes in the Monte Carlo model that match the $\Delta^{17}O(SO_4^{2-})$ observations from 1837–2005 CE (Fig. 6b; red and yellow regions). At a pH of 5.0, there is a linear relationship between changes in $[O_3]$ and $[OH]$. At a higher pH, when O_3 dominates, $\Delta^{17}O(SO_4^{2-})$ is less sensitive to oxidant changes. Ice core observations suggest a pH of Antarctic precipitation of 5.4 (Cragin et al., 1987), however it is difficult to directly link ice core acidity to cloud pH. Snow precipitation may overestimate cloud water pH due to dilution of $[H^+]$ in large droplets. On the other hand, "bulk" cloud water chemistry schemes can underestimate cloud water pH of large droplets, effectively underestimating the importance of O_3 in sulfate formation and $\Delta^{17}O(SO_4^{2-})$ (Roelofs, 1993). Better observational constraints on cloud water pH and $\Delta^{17}O(O_3)$ may improve the ability of $\Delta^{17}O(SO_4^{2-})$ to be used to constrain $[O_3]$ on this time period. That said, the model does suggest that changes in $[O_3]$ of 100 % since the late-1800s, as inferred from remote Southern Hemisphere Schönbein measurements (Sandroni et al., 1992), while not impossible, are difficult to reconcile with the ice core record of $\Delta^{17}O(SO_4^{2-})$, given our present understanding of sulfate formation mechanisms.

6.4 Impact of reactive halogens on $\Delta^{17}O$

Reactive halogens may also impact the formation of both sulfate and nitrate, and hence, their $\Delta^{17}O$. There is no observation-based information about how the abundance of reactive halogens has changed in the recent past. Here we examine the sensitivity of

sulfate and nitrate $\Delta^{17}O$ and our above conclusions regarding oxidant abundances to reactive halogens.

Including $1\,\mathrm{pmol\,mol^{-1}}$ BrO as an oxidant of both NO and NO_2 increases the sensitivity of $\Delta^{17}O(NO_3^-)$ to changes in other oxidants (Fig. 5). If [OH] does not change between 1863–2000 CE, then including BrO in NO_x cycling slightly reduces the fractional decrease in $[O_3]/[RO_2]$ (-46 to $-79\,\%$) required to match the observed change in $\Delta^{17}O(NO_3^-)$. This is because oxidation by BrO is a high-$\Delta^{17}O$ pathway, and with increases in $[O_3]$ and $[RO_2]$, the relative importance of BrO declines, reducing $\Delta^{17}O(NO_3^-)$. However, reactive Br will also reduce $[O_3]$ through its catalytic destruction. While this could potentially further alter $\Delta^{17}O(NO_2)$, the changes associated with NO_x-cycling have little impact on $\Delta^{17}O$, as $NO+O_3$ and $NO+BrO$ have similar isotopic signatures (Savarino et al., 2013). Including BrO also introduces another daytime nitrate formation pathway ($BrONO_2$ hydrolysis), which increases the sensitivity of $\Delta^{17}O(NO_3^-)$ to changes in [OH], partially offsetting the impact of BrO+NO on the sensitivity of $\Delta^{17}O(NO_3^-)$ to changes in $[O_3]/[RO_2]$. If we assume the largest decrease in [OH] from global models ($-33\,\%$) and no other oxidant changes, $\Delta^{17}O(NO_3^-)$ increases by $1.8\,\permil$ due to the increased importance of $BrONO_2$ hydrolysis in nitrate formation. If BrO decreases, the primary impact on $\Delta^{17}O(NO_3^-)$ is a decrease due to the decreased importance of the $BrONO_2$ hydrolysis pathway; the changes associated with NO_x-cycling have little impact on $\Delta^{17}O(NO_3^-)$, as $NO+O_3$ and $NO+BrO$ have similar isotopic signatures (Savarino et al., 2013).

Introducing a fixed concentration of HOCl and HOBr in the sulfate box model reduces the sensitivity of $\Delta^{17}O(SO_4^{2-})$ to changes in other oxidants. Inclusion of this low-$\Delta^{17}O$ aqueous-phase pathway reduces the fraction of sulfate formed by O_3 in both periods, requiring even larger changes in O_3 to match the $\Delta^{17}O(SO_4^{2-})$ observations. On the other hand, at very low concentrations of HOCl and HOBr ($<\sim 2\,\mathrm{pmol\,mol^{-1}}$), $\Delta^{17}O(SO_4^{2-})$ is highly sensitive to changes in [HOCl] or [HOBr], with a halving in [HOCl]

or [HOBr] causing a 1‰ increase in $\Delta^{17}O(SO_4^{2-})$. At higher [HOCl] or [HOBr], these oxidants dominate aqueous-phase sulfate production, leading to very low $\Delta^{17}O(SO_4^{2-})$ values and little change in $\Delta^{17}O(SO_4^{2-})$ with changing [HOCl] or [HOBr] (or other oxidants).

Interestingly, a decrease in the abundance of reactive halogens can qualitatively explain the observed trends in $\Delta^{17}O(SO_4^{2-})$, $\Delta^{17}O(NO_3^-)$, and [MSA]/[nssSO_4^{2-}] in the most recent part of the record. However, there is little information about the variability in reactive halogens on this timescale. Murray et al. (2013), using the reactive bromine chemistry scheme of Parrella et al. (2012) in the GEOS-Chem global chemical transport model, suggests a small increase in [BrO_x] ($BrO_x = Br + BrO$), but the production mechanisms in the model are highly parameterized and do not include potentially important anthropogenic impacts such as changes in pH. However, ice core observations suggest little change in acidity in the high southern latitudes on this time period. The $\Delta^{17}O$ observations will be worth revisiting should new observational and modeling constraints on past reactive halogen abundances be developed.

7 Conclusions

We have measured the $\Delta^{17}O(SO_4^{2-})$, $\Delta^{17}O(NO_3^-)$, and $\delta^{15}N(NO_3^-)$ from the upper 577 m of the WAIS Divide ice cores, spanning ~ 2400 yr. Based on comparison to other ice core observations, we demonstrate that long-term increase in $\delta^{15}N(NO_3^-)$ and decrease in $\Delta^{17}O(NO_3^-)$ can be explained by the impact of the long-term decrease in the snow accumulation rate on the postdepositional loss of snowpack nitrate. However, changes in postdepositional processing cannot explain the 5.6‰ decrease in $\Delta^{17}O(NO_3^-)$ since 1860 CE. The 5.6‰ downward trend in $\Delta^{17}O(NO_3^-)$ since 1860 suggests an increase in the importance of RO_2 relative to O_3 in the oxidation of NO, while there is no apparent change in the formation of nitrate ($NO_2 \rightarrow HNO_3$). The decrease in $\Delta^{17}O(NO_3^-)$ can be explained by a 48–84 % decrease in the [O_3]/[RO_2] ratio in extrat-

ropical Southern Hemisphere NO_x source regions, which is qualitatively consistent with our expectations based on global modeling studies. A decrease in the importance of O_3 relative to RO_2 in NO_x-cycling also leads to an enhancement in the production of O_3 by NO_x-cycling. The 1.1 ‰ step increase in $\Delta^{17}O(SO_4^{2-})$ in the early 19th c. suggests a sustained increase in aqueous-phase sulfate production by O_3 (with an additional 12–18 % of sulfate being formed by O_3) compared to gas-phase production by OH, reducing the fraction of sulfate that can contribute to new particle formation over the Southern Ocean. However, the 210 % increase in $[O_3]/[OH]$ required to explain the observed increase in $\Delta^{17}O(SO_4^{2-})$ in the early 19th c. is much too large to be reconciled with a 26 % increase $[O_3]/[OH]$ from a CTM estimate for the Southern Hemisphere extratropics. This suggests deficiencies in our understanding of remote marine boundary layer sulfate formation, possibly related to sulfate formation involving hypohalous acids (HOCl and HOBr). Observations in the remote MBL of cloud water acidity and hypohalous acids in addition to $\Delta^{17}O(SO_4^{2-})$ may lead to a better understanding of sulfate formation in the remote MBL and shed light on the record of $\Delta^{17}O(SO_4^{2-})$ from the WAIS Divide ice core.

Appendix A

GEOS-Chem Sensitivity Studies

Global model studies report anthropogenic impacts on tropospheric oxidants due to the combined total changes in emissions of CH_4, CO, VOCs, and NO_x between a preindustrial period (typically 1750–1850) and the present (typically 1985–2010). However, emissions of different oxidant precursors (CH_4, CO, VOCs, NO_x) have some independence in their variability over this time period. For example, changes in wetlands will impact CH_4 without impacting NO_x. $[CH_4]$ began increasing around 1800 CE (Mitchell et al., 2011), prior to changes in other oxidant precursors due to anthropogenic ac-

tivity. To investigate how possible emissions changes could impact oxidants since the priendustrial period, we conduct emissions sensitivity studies in which emissions of NO_x, CO, VOCs, or the concentration of CH_4 are independently doubled relative to those in a preindustrial simulation in the GEOS-Chem global three-dimensional at-

5 mospheric chemistry model (Bey et al., 2001; Sofen et al., 2011). The model uses present-day GEOS-4 meteorology. Anthropogenic emissions are turned off and $[CH_4]$ is set to a preindustrial value of $792\,nmol\,mol^{-1}$.

The evolution of preindustrial Southern Hemisphere NO_x, CO, and VOC emissions and concentrations and their impact on oxidants are highly uncertain. The magnitude

10 of the changes in CH_4 and NO_x are similar to the expected changes between the preindustrial and present-day periods, but CO and VOC emissions sensitivity studies likely overestimate actual changes in their emissions. Figure A.A1 shows the percent change in Southern Hemisphere extratropical lower-tropospheric (5 vertical levels; $\sim 2\,km$) annual mean oxidant concentration for each sensitivity study. Doubling the

15 $[CH_4]$ causes increases in O_3 (+9 %) and HO_2 (+10 %), and a decrease in OH (−14 %) in the Southern Hemisphere extratropical lower troposphere. It causes an even larger increase in H_2O_2 (+22 %). A portion of the change in oxidants due to doubling $[CH_4]$ is due to the change in CO that is an oxidation byproduct of the CH_4 and is shown in the hatched portion of the bar chart. Increasing $[CH_4]$ prior to changes in other emissions

20 is qualitatively consistent with the increase in $[O_3]$ and decrease in [OH] suggested by $\Delta^{17}O(SO_4^{2-})$. However, a doubling in $[CH_4]$ (Fig. A1), and certainly the relatively small change in $[CH_4]$ by the mid-1800s, is not enough to produce the magnitude of $[O_3]/[OH]$ changes inferred from $\Delta^{17}O(SO_4^{2-})$.

Most CTMs assume that preindustrial biomass burning CO emissions were 10 % of

25 those in the present-day, but recent ice core and firn air observations of CO isotopes and concentration suggest that Southern Hemisphere [CO] varied widely over the past millennium, including periods when [CO] was higher than in the present day (Wang et al., 2010). Doubling CO emissions causes a small increases in O_3 (+1 %) and HO_2 (+2 %), a small decrease in OH (−3 %) and a larger increase in H_2O_2 (+5 %).

Title Page

Abstract | Introduction

Conclusions | References

Tables | Figures

◄ | ►►

◄ | ►

Back | Close

Full Screen / Esc

Printer-friendly Version

Interactive Discussion

Doubling NO_x emissions increases Southern Hemisphere extratropical O_3 (+6 %) and OH (+8 %) with little influence on HO_2 or H_2O_2 (< 1 %). Emissions inventories suggest that increases in Southern Hemisphere NO_x emissions are likely restricted to the low latitudes (van Aardenne et al., 2001). Similarly, we see no change in $[NO_3^-]$ in the WAIS Divide ice core. However, NO_x emissions at low latitudes may have a larger hemispheric influence on O_3, as O_3 has a longer lifetime than NO_x itself.

We find that increasing VOC emissions produces large increases in HO_2 (+10 %) and H_2O_2 (+31 %), a decrease in OH (– 15 %), and little change in O_3 (–1 %) (because the Southern Hemisphere extra tropics are NO_x-limited). One model study of preindustrial VOC emissions suggests that while on the global scale emissions of isoprene decreased and monoterpenes increased between 1854 and 2000 CE, South American emissions of both VOCs increased, but only by ~ 10 % (Tanaka et al., 2012).

The largest changes in oxidant ratios are a 26 % increase in $[O_3]/[OH]$ due to doubling $[CH_4]$ and a 9 % decrease in $[O_3]/[HO_2]$ due to doubling VOCs. Considering the likely impact of these emissions scenarios on 1800s oxidants, estimated emissions changes in the Southern Hemisphere are likely too small to produce the large oxidant changes suggested by $\Delta^{17}O(SO_4^{2-})$, making it difficult to reconcile CTMs with the oxidant changes implied by the ice core $\Delta^{17}O(SO_4^{2-})$. It is difficult to directly compare the oxidants implied by $\Delta^{17}O(NO_3^-)$ to CTMs because $[RO_2]$ is not typically diagnosed in global models.

References

Alexander, B., Park, R. J., Jacob, D. J., and Gong, S.: Transition metal-catalyzed oxidation of atmospheric sulfur: global implications for the sulfur budget, J. Geophys. Res., 114, D02309, doi:10.1029/2008JD010486, 2009. 23095, 23102, 23104, 23108

Alexander, B., Allman, D. J., Amos, H. M., Fairlie, T. D., Dachs, J., Hegg, D. A., and Sletten, R. S.: Isotopic constraints on the formation pathways of sulfate aerosol in the marine boundary layer of the subtropical northeast Atlantic Ocean, J. Geophys. Res., 117, D06304, doi:10.1029/2011JD016773, 2012. 23094, 23102, 23104

Arsene, C., Barnes, I., and H. Becker, K.: FT-IR product study of the photo-oxidation of dimethyl sulfide: temperature and O_2 partial pressure dependence, Phys. Chem. Chem. Phys., 1, 5463–5470, doi:10.1039/A907211J, 1999. 23095

Barkan, E. and Luz, B.: High precision measurements of $^{17}O/^{16}O$ and $^{18}O/^{16}O$ ratios in H_2O, Rapid Commun. Mass. Sp., 19, 3737–42, doi:10.1002/rcm.2250, 2005. 23095

Bates, T. S., Lamb, B. K., Guenther, A., Dignon, J., and Stoiber, R. E.: Sulfur emissions to the atmosphere from natural sources, J. Atmos. Chem., 14, 315–37, doi:10.1007/BF00115242, 10.1007/BF00115242, 1992. 23095

Beine, H. J. and Krognes, T.: The seasonal cycle of peroxyacetyl nitrate (PAN) in the European Arctic, Atmos. Environ., 34, 933–940, doi:10.1016/S1352-2310(99)00288-5, 2000. 23111

Bey, I., Jacob, D. J., Yantosca, R. M., Logan, J. A., Field, B. D., Fiore, A. M., Li, Q., Liu, H. Y., Mickley, L. J., and Schultz, M. G.: Global modeling of tropospheric chemistry with assimilated meteorology: model description and evaluation, J. Geophys. Res., 106, 23073, doi:10.1029/2001JD000807, 2001. 23121

Blunier, T., Floch, G. L., Jacobi, H.-W., and Quansah, E.: Isotopic view on nitrate loss in Antarctic surface snow, Geophys. Res. Lett., 32, 13501, doi:10.1029/2005GL023011, 2005. 23098

Brenninkmeijer, C. A. M., Janssen, C., Kaiser, J., Röckmann, T., Rhee, T. S., and Assonov, S. S.: Isotope effects in the chemistry of atmospheric trace compounds, Chem. Rev., 103, 5125–5162, doi:10.1021/cr020644k, 2003. 23094

Bretherton, C. S., Widmann, M., Dymnikov, V. P., Wallace, J. M., and Bladé, I.: The effective number of spatial degrees of freedom of a time-varying field, J. Climate, 12, 1990–2009, doi:10.1175/1520-0442(1999)012<1990:TENOSD>2.0.CO;2, 1999. 23107

Cosme, E., Hourdin, F., Genthon, C., and Martinerie, P.: Origin of dimethylsulfide, non-sea-salt sulfate, and methanesulfonic acid in eastern Antarctica, J. Geophys. Res., 110, 3302, doi:10.1029/2004JD004881, 2005. 23113

Cragin, J. H., Giovinetto, M. B., and Gow, A. J.: Baseline acidity of precipitation at the South Pole during the last two millennia, Geophys. Res. Lett., 14, 789–792, doi:10.1029/GL014i008p00789, 1987. 23117

Dubey, M. K., Mohrschladt, R., Donahue, N. M., and Anderson, J. G.: Isotope specific kinetics of hydroxyl radical (OH) with water (H_2O): testing models of reactivity and atmospheric fractionation, J. Phys. Chem. A, 101, 1494–1500, doi:10.1021/jp962332p, 1997. 23095

Eastman, R., Warren, S. G., and Hahn, C. J.: Variations in cloud cover and cloud types over the ocean from surface observations, 1954–2008, J. Climate, 24, 5914–5934, doi:10.1175/2011JCLI3972.1, 2011. 23103

Erbland, J., Vicars, W. C., Savarino, J., Morin, S., Frey, M. M., Frosini, D., Vince, E., and Martins, J. M. F.: Air–snow transfer of nitrate on the East Antarctic Plateau – Part 1: Isotopic evidence for a photolytically driven dynamic equilibrium in summer, Atmos. Chem. Phys., 13, 6403–6419, doi:10.5194/acp-13-6403-2013, 2013. 23098

Faloona, I.: Sulfur processing in the marine atmospheric boundary layer: a review and critical assessment of modeling uncertainties, Atmos. Environ., 43, 2841–2854, doi:10.1016/j.atmosenv.2009.02.043, 2009. 23103

Fegyveresi, J., Alley, R., Spencer, M., Fitzpatrick, J., Steig, E., White, J., McConnell, J., and Taylor, K.: Late-Holocene climate evolution at the WAIS Divide site, West Antarctica: bubble number-density estimates, J. Glaciol., 57, 629–38, doi:10.3189/002214311797409677, 2011. 23106, 23111

Felix, J. D., Elliott, E. M., and Shaw, S. L.: Nitrogen isotopic composition of coal-fired power plant NO_x: influence of emission controls and implications for global emission inventories, Environ. Sci. Technol., 46, 3528–3535, doi:10.1021/es203355v, 2012. 23098, 23112

Fibiger, D. and Hastings, M.: Quantifying the isotopic composition of NO_x emission sources: an analysis of collection methods, in: EGU General Assembly Conference Abstracts, edited by: Abbasi, A., and Giesen, N., no. EGU2012-10816 in Geophysical Research Abstracts, p. 10816, European Geosciences Union, Vienna, Austria, 2012. 23098

Fogelman, K. D., Walker, D. M., and Margerum, D. W.: Non-metal redox kinetics – hypochlorite and hypochlorous acid reactions with sulfite, Inorg. Chem., 28, 986–993, doi:10.1021/ic00305a002, 1989. 23096, 23102

Frey, M. M., Savarino, J., Morin, S., Erbland, J., and Martins, J. M. F.: Photolysis imprint in the nitrate stable isotope signal in snow and atmosphere of East Antarctica and implications for reactive nitrogen cycling, Atmos. Chem. Phys., 9, 8681–8696, doi:10.5194/acp-9-8681-2009, 2009. 23098, 23100

5 Hastings, M. G.: Evaluating source, chemistry and climate change based upon the isotopic composition of nitrate in ice cores, IOPC Ser. Earth Env., 9, 012002, doi:10.1088/1755-1315/9/1/012002, 2010. 23106

Hastings, M. G., Steig, E. J., and Sigman, D. M.: Seasonal variations in N and O isotopes of nitrate in snow at Summit, Greenland: implications for the study of nitrate in snow and ice
10 cores, J. Geophys. Res., 109, D20306, doi:10.1029/2004JD004991, 2004. 23112

Hastings, M. G., Jarvis, J. C., and Steig, E. J.: Anthropogenic impacts on nitrogen isotopes of ice-core nitrate, Science, 324, 1288, doi:10.1126/science.1170510, 2009. 23112

Holland, H. D.: The Chemistry of the Atmosphere and Oceans, chap. 5, John Wiley & Sons, Inc., New York, 1978. 23101

15 Holmes, C. D., Prather, M. J., Søvde, O. A., and Myhre, G.: Future methane, hydroxyl, and their uncertainties: key climate and emission parameters for future predictions, Atmos. Chem. Phys., 13, 285–302, doi:10.5194/acp-13-285-2013, 2013. 23093

Jacobi, H.-W., Weller, R., Jones, A., Anderson, P., and Schrems, O.: Peroxyacetyl nitrate (PAN) concentrations in the Antarctic troposphere measured during the photochemical ex-
20 periment at Neumayer (PEAN'99), Atmos. Environ., 34, 5235–5247, doi:10.1016/S1352-2310(00)00190-4, 2000. 23111

John, J. G., Fiore, A. M., Naik, V., Horowitz, L. W., and Dunne, J. P.: Climate versus emission drivers of methane lifetime against loss by tropospheric OH from 1860–2100, Atmos. Chem. Phys., 12, 12021–12036, doi:10.5194/acp-12-12021-2012, 2012. 23093

25 Johnston, J. C. and Thiemens, M. H.: The isotopic composition of tropospheric ozone in three environments, J. Geophys. Res., 102, 25395–25404, doi:10.1029/97JD02075, 1997. 23094

Jones, A. E., Wolff, E. W., Ames, D., Bauguitte, S. J.-B., Clemitshaw, K. C., Fleming, Z., Mills, G. P., Saiz-Lopez, A., Salmon, R. A., Sturges, W. T., and Worton, D. R.: The multi-seasonal NO_y budget in coastal Antarctica and its link with surface snow and ice core nitrate:
30 results from the CHABLIS campaign, Atmos. Chem. Phys., 11, 9271–9285, doi:10.5194/acp-11-9271-2011, 2011. 23111

Title Page

Abstract | Introduction

Conclusions | References

Tables | Figures

◀ | ▶

◀ | ▶

Back | Close

Full Screen / Esc

Printer-friendly Version

Interactive Discussion

Kaiser, J., Hastings, M. G., Houlton, B. Z., Röckmann, T., and Sigman, D. M.: Triple oxygen isotope analysis of nitrate using the denitrifier method and thermal decomposition of N_2O, Anal. Chem., 79, 599–607, doi:10.1021/ac061022s, 2007. 23100

Kaufman, Y. and Tanre, D.: Effect of variations in super-saturation on the formation of cloud condensation nuclei, Nature, 369, 45–48, doi:10.1038/369045a0, 1994. 23092

Krankowsky, D., Bartecki, F., Klees, G. G., Mauersberger, K., and Schellenbach, K.: Measurement of heavy isotope enrichment in tropospheric ozone, Geophys. Res. Lett., 22, 1713–1716, doi:10.1029/95GL01436, 1995. 23094

Kunasek, S. A., Alexander, B., Steig, E. J., Hastings, M. G., Gleason, D. J., and Jarvis, J. C.: Measurements and modeling of $\Delta^{17}O$ of nitrate in snowpits from Summit, Greenland, J. Geophys. Res., 113, D24302, doi:10.1029/2008JD010103, 2008. 23102

Kunasek, S. A., Alexander, B., Steig, E. J., Sofen, E. D., Jackson, T. L., Thiemens, M. H., McConnell, J. R., Gleason, D. J., and Amos, H. M.: Sulfate sources and oxidation chemistry over the past ∼ 230 years from sulfur and oxygen isotopes of sulfate in a West Antarctic ice core, J. Geophys. Res., 115, D18313, doi:10.1029/2010JD013846, 2010. 23094, 23099, 23101, 23105, 23117

Lamarque, J.-F., Mcconnell, J. R., Shindell, D. T., Orlando, J. J., and Tyndall, G. S.: Understanding the drivers for the 20th century change of hydrogen peroxide in Antarctic ice-cores, Geophys. Res. Lett., 38, L04810, doi:10.1029/2010GL045992, 2011. 23093, 23109

Langner, J., Rodhe, H., Crutzen, P. J., and Zimmermann, P.: Anthropogenic influence on the distribution of tropospheric sulphate aerosol, Nature, 359, 712–716, doi:10.1038/359712a0, 1992. 23092

Liu, Q.: Kinetics of aqueous phase reactions related to ozone depletion in the Arctic troposphere: bromine chloride hydrolysis, bromide ion with ozone, and sulfur((IV)) with bromine and hypobromous acid, Ph.D. thesis, Purdue University, Lafayette, IN, 2002. 23095

Lyons, J. R.: Transfer of mass-independent fractionation in ozone to other oxygen-containing radicals in the atmosphere, Geophys. Res. Lett., 28, 3231–3234, doi:10.1029/2000GL012791, 2001. 23094, 23095

Masclin, S., Frey, M. M., Rogge, W. F., and Bales, R. C.: Atmospheric nitric oxide and ozone at the WAIS Divide deep coring site: a discussion of local sources and transport in West Antarctica, Atmos. Chem. Phys. Discuss., 13, 6807–6849, doi:10.5194/acpd-13-6807-2013, 2013. 23097

McGwire, K. C., Taylor, K. C., Banta, J. R., and McConnell, J. R.: Identifying annual peaks in dielectric profiles with a selection curve, J. Glaciol., 57, 763–769, doi:10.3189/002214311797409721, 2011. 23099

Michalski, G., Scott, Z., Kabiling, M., and Thiemens, M. H.: First measurements and modeling of Δ^{17}O in atmospheric nitrate, J. Geophys. Res., 30, 1870, doi:10.1029/2003GL017015, 2003. 23094, 23095

Mitchell, L. E., Brook, E. J., Sowers, T., Mcconnell, J. R., and Taylor, K.: Multidecadal variability of atmospheric methane, 1000–1800 C. E., J. Geophys. Res., 116, G02007, doi:10.1029/2010JG001441, 2011. 23120

Morin, S., Savarino, J., Bekki, S., Gong, S., and Bottenheim, J. W.: Signature of Arctic surface ozone depletion events in the isotope anomaly (Δ^{17}O) of atmospheric nitrate, Atmos. Chem. Phys., 7, 1451–1469, doi:10.5194/acp-7-1451-2007, 2007. 23092, 23094, 23095

Morin, S., Savarino, J., Frey, M. M., Domine, F., Jacobi, H.-W., Kaleschke, L., and Martins, J. M. F.: Comprehensive isotopic composition of atmospheric nitrate in the Atlantic Ocean boundary layer from 65°S to 79°N, J. Geophys. Res., 114, D05303, doi:10.1029/2008JD010696, 2009. 23098, 23112

Morin, S., Sander, R., and Savarino, J.: Simulation of the diurnal variations of the oxygen isotope anomaly (Δ^{17}O) of reactive atmospheric species, Atmos. Chem. Phys., 11, 3653–3671, doi:10.5194/acp-11-3653-2011, 2011. 23094

Murray, L. T., Mickley, L. J., Kaplan, J. O., Sofen, E. D., Pfeiffer, M., and Alexander, B.: Factors controlling variability in the oxidative capacity of the troposphere since the Last Glacial Maximum, Atmos. Chem. Phys. Discuss., in press, 2013. 23119

Parish, T. R. and Bromwich, D. H.: Reexamination of the near-surface airflow over the Antarctic continent and implications on atmospheric circulations at high southern latitudes, Mon. Weather Rev., 135, 1961–1973, doi:10.1175/MWR3374.1, 2007. 23097

Park, R. J., Jacob, D. J., Field, B. D., Yantosca, R. M., and Chin, M.: Natural and transboundary pollution influences on sulfate-nitrate-ammonium aerosols in the United States: implications for policy, J. Geophys. Res., 109, D15204, doi:10.1029/2003JD004473, 2004. 23096

Parrella, J. P., Jacob, D. J., Liang, Q., Zhang, Y., Mickley, L. J., Miller, B., Evans, M. J., Yang, X., Pyle, J. A., Theys, N., and Van Roozendael, M.: Tropospheric bromine chemistry: implications for present and pre-industrial ozone and mercury, Atmos. Chem. Phys., 12, 6723–6740, doi:10.5194/acp-12-6723-2012, 2012. 23119

WAIS Divide sulfate and nitrate isotopes

E. D. Sofen et al.

Pasteris, D. R., McConnell, J. R., and Edwards, R.: High-resolution, continuous method for measurement of acidity in ice cores, Environ. Sci. Technol., 46, 1659–1666, doi:10.1021/es202668n, 2012. 23112

Patris, N., Delmas, R. J., and Jouzel, J.: Isotopic signatures of sulfur in shallow Antarctic ice cores, J. Geophys. Res., 105, 7071–7078, doi:10.1029/1999JD900974, 2000. 23113

Pavelin, E. G., Johnson, C. E., Rughooputh, S., and Toumi, R.: Evaluation of pre-industrial surface ozone measurements made using Schönbein's method, Atmos. Environ., 33, 919–929, doi:10.1016/S1352-2310(98)00257-X, 1999. 23093

Read, K. A., Lewis, A. C., Bauguitte, S., Rankin, A. M., Salmon, R. A., Wolff, E. W., Saiz-Lopez, A., Bloss, W. J., Heard, D. E., Lee, J. D., and Plane, J. M. C.: DMS and MSA measurements in the Antarctic Boundary Layer: impact of BrO on MSA production, Atmos. Chem. Phys., 8, 2985–2997, doi:10.5194/acp-8-2985-2008, 2008. 23095

Roelofs, G.: A cloud chemistry sensitivity study and comparison of explicit and bulk cloud model performance, Atmos. Environ., 27, 2255–2264, doi:10.1016/0960-1686(93)90396-G, 1993. 23117

Saiz-Lopez, A. and von Glasow, R.: Reactive halogen chemistry in the troposphere, Chem. Soc. Rev., 41, 6448–6472, doi:10.1039/C2CS35208G, 2012. 23092

Salawitch, R. J., Gobbi, G. P., Wofsy, S. C., and McElroy, M. B.: Denitrification in the Antarctic stratosphere, Nature, 339, 525–527, doi:10.1038/339525a0, 1989. 23096

Sandroni, S., Anfossi, D., and Viarengo, S.: Surface ozone levels at the end of the nineteenth century in South America, J. Geophys. Res., 97, 2535–2539, 1992. 23093, 23117

Savarino, J. and Thiemens, M. H.: Analytical procedure to determine both $\delta^{18}O$ and $\delta^{17}O$ of H_2O_2 in natural water and first measurements, Atmos. Environ., 33, 3683–3690, doi:10.1016/S1352-2310(99)00122-3, 1999. 23095

Savarino, J., Lee, C. C. W., and Thiemens, M. H.: Laboratory oxygen isotopic study of sulfur(IV) oxidation: origin of the mass-independent oxygen isotopic anomaly in atmospheric sulfates and sulfate mineral deposits on Earth, J. Geophys. Res., 106, 29079–29088, doi:10.1029/2000JD900456, 2000. 23095

Savarino, J., Alexander, B., Darmohusodo, V., and Thiemens, M. H.: Sulfur and oxygen isotope analysis of sulfate at micromole levels using a pyrolysis technique in a continuous flow system, Anal. Chem., 73, 4457–4462, 2001. 23101

Title Page

Abstract | Introduction

Conclusions | References

Tables | Figures

◄ | ►

◄ | ►

Back | Close

Full Screen / Esc

Printer-friendly Version

Interactive Discussion

Savarino, J., Kaiser, J., Morin, S., Sigman, D. M., and Thiemens, M. H.: Nitrogen and oxygen isotopic constraints on the origin of atmospheric nitrate in coastal Antarctica, Atmos. Chem. Phys., 7, 1925–1945, doi:10.5194/acp-7-1925-2007, 2007. 23096, 23098

Savarino, J., Morin, S., Erbland, J., Grannec, F., Patey, M. D., Vicars, W., Alexander, B., and Achterberg, E. P.: Isotopic composition of atmospheric nitrate in a tropical marine boundary layer, P. Natl. Acad. Sci. USA, doi:10.1073/pnas.1216639110, 2013. 23118

Schauer, A. J., Kunasek, S. A., Sofen, E. D., Erbland, J., Savarino, J., Johnson, B. W., Amos, H. M., Shaheen, R., Abaunza, M., Jackson, T. L., Thiemens, M. H., and Alexander, B.: Oxygen isotope exchange with quartz during pyrolysis of silver sulfate and silver nitrate, Rapid Commun. Mass. Sp., 26, 2151–2157, doi:10.1002/rcm.6332, 2012. 23101

Seinfeld, J. H. and Pandis, S. N.: Atmospheric Chemistry and Physics: From Air Pollution to Climate Change, 2nd edn., John Wiley & Sons, Inc., Hoboken, NJ, 2006. 23095, 23104

Sigman, D. M., Casciotti, K. L., Andreani, M., Barford, C., Galanter, M., and Böhlke, J. K.: A bacterial method for the nitrogen isotopic analysis of nitrate in seawater and freshwater, Anal. Chem., 73, 4145–4153, doi:10.1021/ac010088e, 2001. 23100

Sofen, E. D., Alexander, B., and Kunasek, S. A.: The impact of anthropogenic emissions on atmospheric sulfate production pathways, oxidants, and ice core $\Delta^{17}O(SO_4^{2-})$, Atmos. Chem. Phys., 11, 3565–3578, doi:10.5194/acp-11-3565-2011, 2011. 23093, 23094, 23108, 23113, 23114, 23117, 23121, 23138

Spiro, P. A., Jacob, D. J., and Logan, J. A.: Global inventory of sulfur emissions with 1° × 1° resolution, J. Geophys. Res., 97, 6023–6036, doi:10.1029/91JD03139, 1992. 23095

Tanaka, K., Kim, H.-J., Saito, K., Takahashi, H. G., Watanabe, M., Yokohata, T., Kimoto, M., Takata, K., and Yasunari, T.: How have both cultivation and warming influenced annual global isoprene and monoterpene emissions since the preindustrial era?, Atmos. Chem. Phys., 12, 9703–9718, doi:10.5194/acp-12-9703-2012, 2012. 23122

Thiemens, M. H.: History and applications of mass-independent isotope effects, Ann. Rev. Earth Pl. Sc., 34, 217–262, doi:10.1146/annurev.earth.34.031405.125026, 2006. 23094

Thiemens, M. H. and Heidenreich, J.: The mass-independent fractionation of oxygen: a novel isotope effect and its possible cosmochemical implications, Science, 219, 1073–1075, doi:10.1126/science.219.4588.1073, 1983. 23094

Troy, R. C. and Margerum, D. W.: Non-metal redox kinetics: Hypobromite and hypobromous acid reactions with iodide and with sulfite and the hydrolysis of bromosulfate, Inorg. Chem., 30, 3538–3543, doi:10.1021/ic00018a028, 1991. 23096, 23102

van Aardenne, J. A., Dentener, F. J., Olivier, J. G. J., Klein Goldewijk, C. G. M., and Lelieveld, J.: A 1° × 1° resolution data set of historical anthropogenic trace gas emissions for the period 1890–1990, Glob. Biogeochem. Cy., 15, 909, doi:10.1029/2000GB001265, 2001. 23122

Vicars, W. C., Bhattacharya, S. K., Erbland, J., and Savarino, J.: Measurement of the [17]O-excess ($\Delta^{17}O$) of tropospheric ozone using a nitrite-coated filter, Rapid Commun. Mass. Sp., 26, 1219–1231, doi:10.1002/rcm.6218, 2012. 23094

Vogt, R., Crutzen, P. J., and Sander, R.: A mechanism for halogen release from sea-salt aerosol in the remote marine boundary layer, Nature, 383, 327–330, doi:10.1038/383327a0, 1996. 23095

von Glasow, R., Sander, R., Bott, A., and Crutzen, P. J.: Modeling halogen chemistry in the marine boundary layer 2. Interactions with sulfur and the cloud-covered MBL, J. Geophys. Res., 107, 4323, doi:10.1029/2001JD000943, 2002. 23095

von Glasow, R., von Kuhlmann, R., Lawrence, M. G., Platt, U., and Crutzen, P. J.: Impact of reactive bromine chemistry in the troposphere, Atmos. Chem. Phys., 4, 2481–2497, doi:10.5194/acp-4-2481-2004, 2004. 23092

Wang, Z., Chappellaz, J., Park, K., and Mak, J. E.: Large variations in Southern Hemisphere biomass burning during the last 650 years, Science, 330, 1663–1666, doi:10.1126/science.1197257, 2010. 23121

Weller, R., Traufetter, F., Fischer, H., Oerter, H., Piel, C., and Miller, H.: Postdepositional losses of methane sulfonate, nitrate, and chloride at the European Project for Ice Coring in Antarctica deep-drilling site in Dronning Maud Land, Antarctica, J. Geophys. Res., 109, D07301, doi:10.1029/2003JD004189, 2004. 23110

Wolff, E. W., Jones, A. E., Bauguitte, S. J.-B., and Salmon, R. A.: The interpretation of spikes and trends in concentration of nitrate in polar ice cores, based on evidence from snow and atmospheric measurements, Atmos. Chem. Phys., 8, 5627–5634, doi:10.5194/acp-8-5627-2008, 2008. 23097, 23111

Xu, L. and Penner, J. E.: Global simulations of nitrate and ammonium aerosols and their radiative effects, Atmos. Chem. Phys., 12, 9479–9504, doi:10.5194/acp-12-9479-2012, 2012. 23097

Zatko, M. C., Grenfell, T. C., Alexander, B., Doherty, S. J., Thomas, J. L., and Yang, X.: The influence of snow grain size and impurities on the vertical profiles of actinic flux and associated NO_x emissions on the Antarctic and Greenland ice sheets, Atmos. Chem. Phys., 13, 3547–3567, doi:10.5194/acp-13-3547-2013, 2013. 23098

WAIS Divide sulfate and nitrate isotopes

E. D. Sofen et al.

Table 1. Ice core sampling resolution and isotopic measurements.

Core	Depth Range (m) Time Range	Depth Res. (m) Time Res. (yr)	#Samples (#Replicates)	Measurements
WDC05A	0–69.8 1774–2005 CE	7.03–12.86 27–44	6 (1)	$\Delta^{17}O(SO_4^{2-})$
WDC05A	0–69.8 1774-2005 CE	0.875–1.12 1.8–4.8	70 (1)	$\delta^{15}N(NO_3^-)$
WDC05Q	0–129.17 1521–2000 CE	0.546–1.37 2.3–6.1	121 (3)	$\Delta^{17}O(NO_3^-)$
WDC06A	114–577 427 BCE–1586 CE	12–15 50–68	32 (1)	$\Delta^{17}O(SO_4^{2-})$
WDC06A	114–577 427 BCE–1586 CE	12–15 50–68	32 (3)	$\Delta^{17}O(NO_3^-)$
WDC06A	114–577 427 BCE–1586 CE	12–15 50–68	32 (3)	$\delta^{15}N(NO_3^-)$
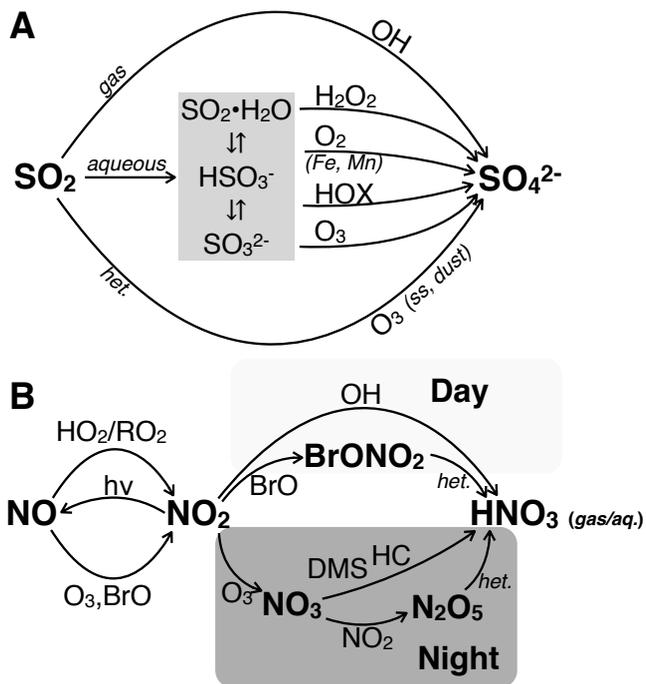
Fig. 1. Summary of major **(A)** sulfate production pathways and **(B)** nitrate production path-ways. "HOX" = HOBr or HOCl; "ss" = sea salt; "het." = heterogeneous reactions on the surface of aerosols. HNO_3 formed through the heterogeneous reactions is formed in the aqueous-phase, while the other pathways produce gas-phase HNO_3. HNO_3 partitions between gas and aqueous phases based on aerosol thermodynamics. Aqueous-phase HNO_3 may dissociate into $H^+ + NO_3^-$.
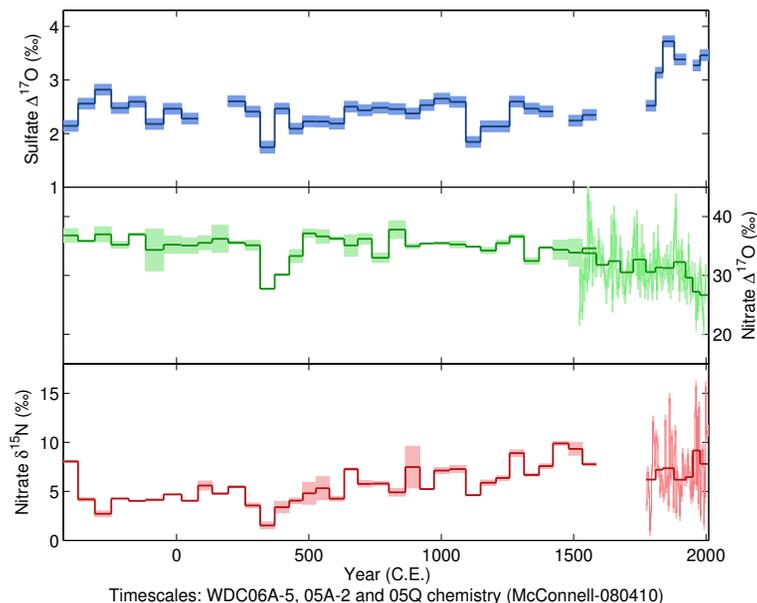
Fig. 2. Measurements of $\Delta^{17}O(SO_4^{2-})$, $\Delta^{17}O(NO_3^-)$, and $\delta^{15}N(NO_3^-)$ in the upper 577 m of the WAIS Divide ice core. Each horizontal line segment indicates the time interval of that sample. Shading indicates the measurement uncertainty based on the replicate analysis of standards ($\Delta^{17}O(SO_4^{2-})$) or replicate sample measurements ($\Delta^{17}O(NO_3^-)$, $\delta^{15}N(NO_3^-)$). The recent part of the nitrate isotope records are measured at 1 m resolution (see Fig. 4 for an expanded version of this record); the thick lines through this portion of the $\Delta^{17}O(NO_3^-)$ and $\delta^{15}N(NO_3^-)$ indicate the concentration-weighted isotopic values at the resolution of the $\Delta^{17}O(SO_4^{2-})$.
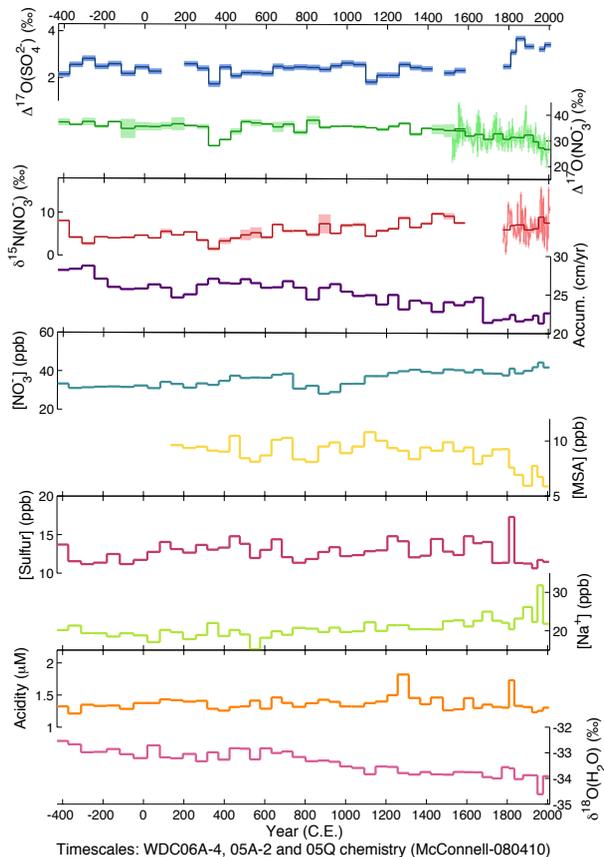
Fig. 3. Low resolution sulfate and nitrate isotopes compared to measurements of accumulation rate, nitrate concentration, MSA concentration, $[MSA]/[nssSO_4^{2-}]$ ratio, sulfur concentration, sodium concentration, acidity, and $\delta^{18}O(H_2O)$ from the WDC06A core (except for $nssSO_4^{2-}$, from WDC05Q) averaged to the resolution of the sulfate isotope data.

Title Page

Abstract | Introduction

Conclusions | References

Tables | Figures

|◄ | ►|

◄ | ►

Back | Close

Full Screen / Esc

Printer-friendly Version

Interactive Discussion
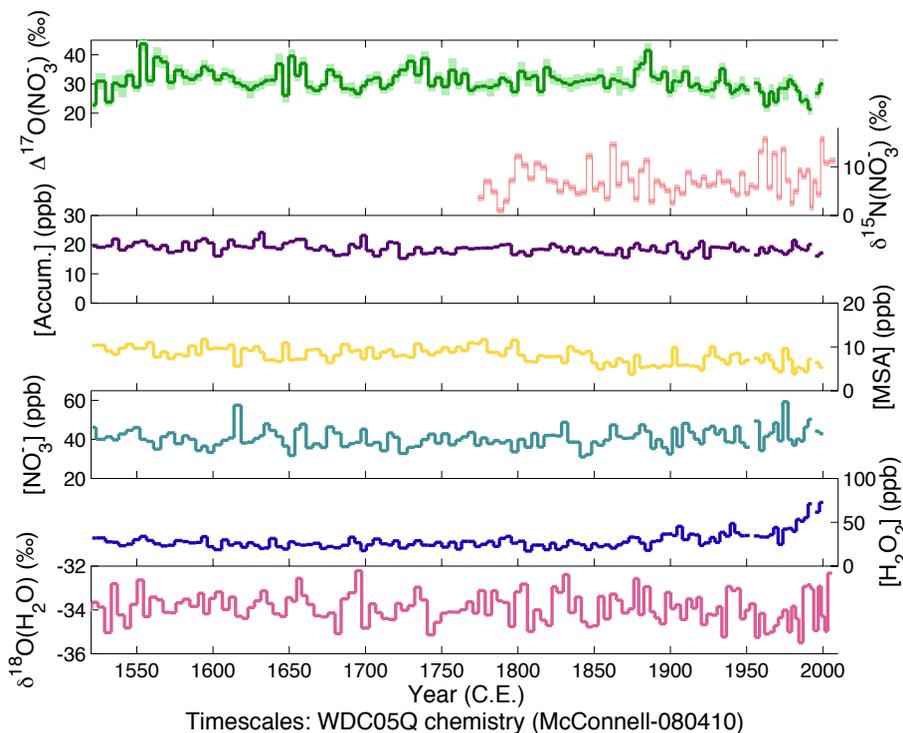
Fig. 4. 1 m resolution $\Delta^{17}O(NO_3^-)$ (WDC05Q core) and $\delta^{15}N(NO_3^-)$ (WDC05A) compared to measurements of accumulation rate (WDC05Q), MSA concentration (WDC06A), nitrate concentration (WDC06A), and hydrogen peroxide concentration (WDC05Q), averaged to the resolution of the $\Delta^{17}O(NO_3^-)$ data. $\delta^{18}O(H_2O)$ is shown at the resolution of the $\delta^{15}N(NO_3^-)$ data, as they were both measured at 1 m resolution on the same core (WDC05A).

Full Screen / Esc
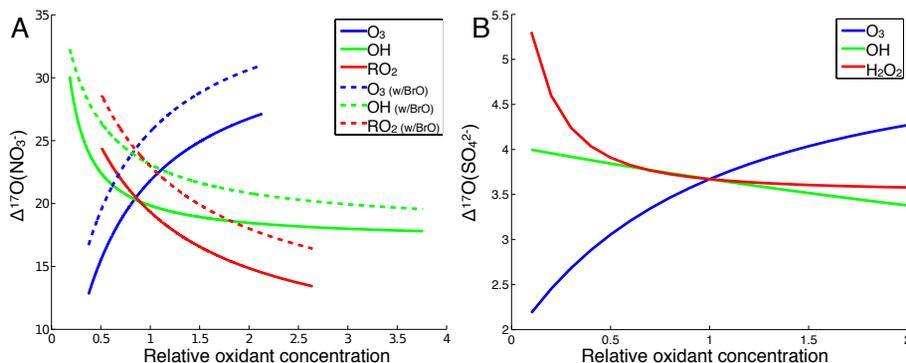
Fig. 5. Sensitivity of **(A)** $\Delta^{17}O(NO_3^-)$ and **(B)** $\Delta^{17}O(SO_4^{2-})$ to variations in each oxidant, normalized to the mean oxidant concentrations of the present-day South American and Southern Ocean boundary layers, respectively. Dashed lines indicate results when $1\,\mathrm{pmol\,mol^{-1}}$ BrO is include as both an oxidant of NO in NO_x-cycling and as an oxidant of NO_2, which leads to nitrate formation via the hydrolysis of $BrONO_2$.
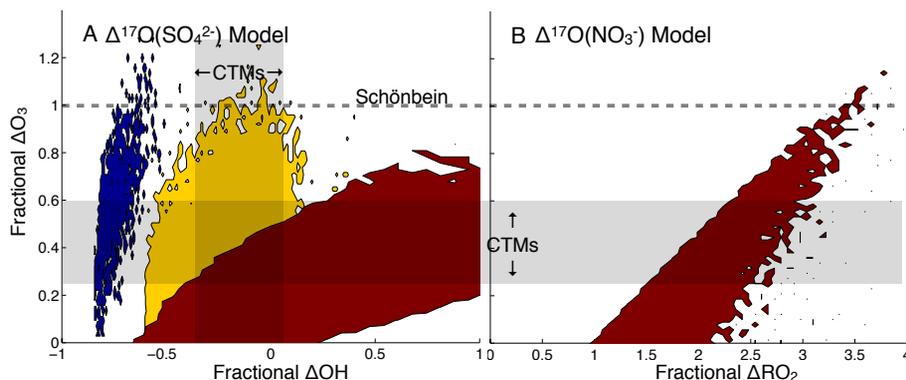
Fig. 6. Envelope of fractional oxidant changes from Monte Carlo simulations matching the observed changes in $\Delta^{17}O$. **(A)** Change in $[O_3]$ and $[OH]$ associated with the early 19th c. increase in $\Delta^{17}O(SO_4^{2-})$ assuming cloud water pH = 5.0–6.0 (blue) and no change in $\Delta^{17}O(SO_4^{2-})$ with a 40–50 % increase in $[H_2O_2]$ between the mid 19th c. and present-day assuming cloud water pH = 5.0 (red) and 6.0 (yellow). **(B)** Changes in $[RO_2]$ and $[O_3]$ matching the 5.6 ‰ decline in $\Delta^{17}O(NO_3^-)$ from the 1860s to present-day assuming ≤ 5 % change in $[OH]$. Grey shading indicate the range of preindustrial to present-day changes in $[O_3]$ and $[OH]$ in global CTMs. The dashed line indicate the late 19th c. to present-day change in $[O_3]$ based on Southern Hemisphere extratropical Schönbein measurements.

Title Page

Abstract | Introduction

Conclusions | References

Tables | Figures

◀ | ▶

◀ | ▶

Back | Close

Full Screen / Esc

Printer-friendly Version

Interactive Discussion
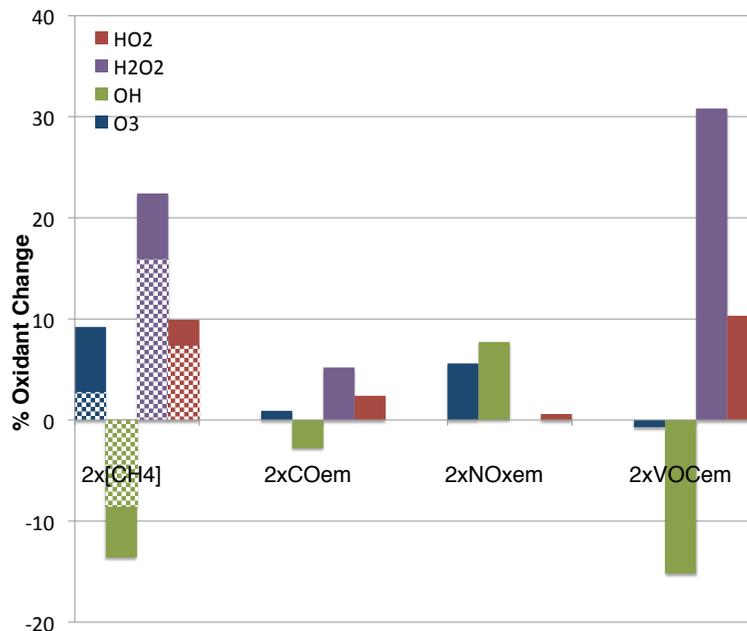
Fig. A1. Sensitivity of oxidant concentrations to a doubling in [CH$_4$] or emissions of CO, NO$_x$, or VOCs relative to a simulation of preindustrial oxidant chemistry (Sofen et al., 2011). Each bar represents the fractional change in Southern Hemisphere extratropical lower tropospheric (≤ 2 km) oxidant concentration. The checkered segment of the CH$_4$ sensitivity study indicates the fraction of the oxidant changes for which CH$_4$-derived CO is responsible.